Universität Hamburg

CHL1 organizes ankyrin-B / βII spectrin based cytoskeleton in developing neurons *(Mus musculus L., 1758)*

DISSERTATION

Von

Nan Tian

zur Erlangung des akademischen Grades Doktor der Naturwissenschaften Dr. rer. nat. am Department Biologie der Fakultät für Mathematik, Informatik und Naturwissenschaften der Universität Hamburg

Hamburg, June 2009

Genehmigt vom Department Biologie
der Fakultät für Mathematik, Informatik und Naturwissenschaften
an der Universität Hamburg
auf Antrag von Frau Professor Dr. M. SCHACHNER
Weiterer Gutachter der Dissertation:
Herr Professor Dr. K. WIESE
Tag der Disputation: 19. Juni 2009

Hamburg, den 05. Juni 2009

Professor Dr. Jörg Ganzhorn
Leiter des Departments Biologie

University of Wisconsin-Madison
Pathology and Laboratory Medicine
1300 University Ave., 6415 MSC
Madison, WI 53706

May 15, 2009

RE: Doctoral Thesis for Nan Tian, University of Hamburg

To Whom It May Concern:

I, DeannaLee M. Beauvais, the undersigned, certify that I am a native English speaker. I have read Nan Tian's draft doctoral thesis and have provided relevant corrections I believe should be incorporated into her final thesis. I affirm that the thesis's general language, grammar and spelling are correct and should be readily understood by any native English speaker.

Sincerely,

DeannaLee M. Beauvais, PhD
Research Associate
University of Wisconsin-Madison

CONTENTS

I ABSTRACT

Close homolog of L1 (CHL1) is a member of the L1 family of cell adhesion molecules， which belongs to the immunoglobulin superfamily. In developing brains, CHL1 regulates neuronal migration and axon outgrowth and guidance. The dynamic regulation of cell adhesion through coupling of adhesion receptors with the cytoskeleton is important for these processes. However, the molecular mechanisms by which CHL1 regulates the cytoskeleton remain poorly investigated. Here we report that CHL1 associates with βII spectrin, a membrane-cytoskeleton linker protein which is involved in membrane stabilization as well as vesicle trafficking, independently of its adaptor ankyrin-B. In brains of young CHL1 deficient mice, targeting of βII spectrin to growth cones is reduced, implicating CHL1 as a growth cone-targeting cue for βII spectrin. CHL1 enhances association of βII spectrin with lipid raft micro-domain. Furthermore, we show that CHL1 antibody-treatment induces internalization of CHL1, which is dependent on Ca^{2+} influx via L-type calcium channels. The association of CHL1 with lipid rafts is required for its internalization and CHL1-dependent detachment of βII spectrin from the plasma membrane. Considering that the polymerization of spectrin meshwork is increased in CHL1 deficient mice, CHL1 may regulate depolymerization of spectrin meshwork through lipid rafts related Ca^{2+} signaling. For the functional study, we demonstrate that CHL1 antibody-application to live cells *in vitro* promotes neurite outgrowth, and this effect is abolished either by pharmacological treatments that deplete cellular cholesterol and sphingolipids, or by mutation of CHL1 at the palmitoylation site, suggesting lipid rafts are important for CHL1 dependent neurite outgrowth. Taken together, our data suggest that the dynamic interaction between βII spectrin and CHL1 dependent on lipid rafts plays a role in CHL1-mediated neurite outgrowth.

Key words: CHL1, ankyrin-B, βII spectrin, lipid rafts, Ca^{2+}, endocytosis, neurite outgrowth,

II AIMS OF THE STUDY

Close homolog of L1 (CHL1) regulates neuronal migration, axon outgrowth and guidance (Maness and Schachner, 2007). The dynamic regulation of cell adhesion through coupling of adhesion receptors with the cytoskeleton is important for these processes. However, the molecular mechanisms by which CHL1 regulates the cytoskeleton remain poorly investigated. In L1 family, the cytoplasmic domain of L1 molecules contains a conserved sequence (FIGQ/AY) that reversibly binds to ankyrin, which couples L1 to the subcortical spectrin mesh-work. The spectrin is recognized as a ubiquitous scaffolding protein that can organize membrane microdomains and link membrane protein to actin/microtubule cytoskeletons (Bennett and Healy, 2008). So we are promoted to investigate the roles of CHL1 in regulating ankyrin/spectrin based cytoskeleton in developing brains.

The aims of this study are:

- to examine the possibility of interaction between CHL1 and ankyrin/spectirn-based cytoskeleton;
- to investigate whether CHL1 regulates the ankyrin/spectrin-based cytoskeleton;
- to determine the functional consequence of the interaction between CHL1 and ankyrin/spectrin-based cytoskeleton.

III INTRODUCTION

During brain development, recognition among neural cells is an important prerequisite for a functioning nervous system. Interactions between neural cells are important for precise regulation and intercellular communication. Cell adhesion molecules (CAMs) are expressed at the cell surface, where they mediate interactions between neighboring cells or between the cell surface and the extracellular matrix. CAMs expressed by neurons can be divided into three large families: integrins, cadherins and the immunoglobulin superfamily (IgSF). Integrins interact heterophilically, i.e., with extracellular matrix molecules, such as laminin (Letourneau et al., 1994). Cadherin and the majority of IgSF CAMs interact homophilically, i.e., with the same type of molecules present on adjacent cells (Takeichi, 1991; Brummendorf and Rathjen, 1994).Some IgCAMs, such as neural cell adhesion molecule (NCAM) and the L1 subfamily, are especially important for nervous system development (Maness and Schachner, 2007).

L1 subfamily includes four members in vertebrate: L1, close homolog of L1 (CHL1), neurofascin, and Nr-CAM (neuron-glia-CAM-related cell adhesion molecule), along with their homologues in other species. The importance of L1 subfamily in neural development, including neuronal migration, neurite outgrowth, synapse formation, myelination and other events during the development of the nervous system, has been revealed in diverse ways. In humans, mutation in the *L1* gene can have devastating consequences. In extreme cases, babies are born with a fatal condition of hydrocephalus (“water on the brain”) (Fransen et al., 1995). Autopsies on patients that have died of an L1-deficiency disease reveal a remarkable abnormality: they are often missing two large nerve tracts, one that runs between the two halves of the brain and the other that runs between the brain and the spinal cord (Kenwrick and Doherty, 1998). The absence of such nerve tracts suggests that L1 is involved in the growth of axons within the

embryonic nervous system. Another prominent member of L1 subfamily, close homolog of L1 (CHL1), is implicated in schizophrenia, mental impairment associated with ‘‘3p-syndrome’’ and mental retardation (Angeloni et al., 1999b; Angeloni et al., 1999a; Frints et al., 2003). The association between CHL1 and various nervous system related disorders emphasizes the importance to understand the cellular functions of this molecule in detail.

III.1 The close homolog of L1

CHL1 was first identified by screening a cDNA library using polyclonal antibodies against brain-derived immunopurified L1 in 1996 (Holm et al., 1996). In the last decade, CHL1 has been revealed many critical roles during brain development, such as neuronal migration and neurite outgrowth.

CHL1 is a transmembrane protein consisting of an extracellular domain, a transmembrane portion and an intracellular domain. The extracellular domain of CHL1 contains six Ig-like domains and four full-length and one rudimentary half-length fibronectin type III (FN)-like repeats (Holm et al., 1996) (Fig. III.1). Each Ig-like domain contains about 70-110 amino acids and possesses a characteristic fold in which two beta sheets form a ‘sandwich’ that is stabilized by an interaction between conserved cysteines (Barclay, 2003). The Ig-like domains reflect the common ancestry of immunoglobulins and cell adhesion molecules, both of which are involved in specific recognition events (Barclay, 2003). FNIII-like repeats are protein domains that are frequently combined with Ig-like domains. Crystallographic analysis reveals a striking structural similarity between the FNIII-like repeat and Ig-like domain. However, in contrast to Ig-like domains, the FNIII-like repeats are usually not stabilized by disulfide bridges (Leahy et al., 1992; Main et al., 1992).

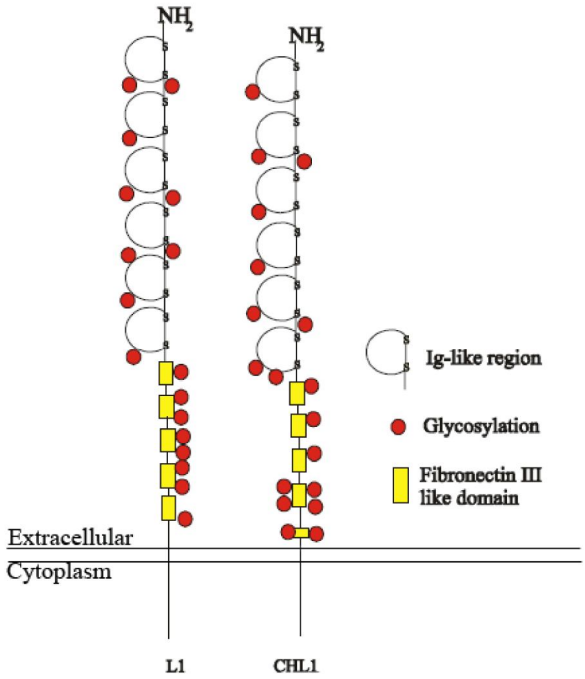

Figure III.1. Schematic structure of L1 and CHL1. L1 and CHL1 show similarity in structure. CHL1 contains six Ig-like domains followed by four and half FNIII-like repeats in the extracellular domain, a short transmembrane region and an intracellular domain. Immunoglobulin, Ig; fibronectin, FN.

Within FNIII-like domains, cell adhesion molecules can be proteolytically processed and released from the cell membrane, which is important for certain biological functions. The transmembrane CHL1 (185 kDa) can be cleavage at FNIII domain II and V to produce soluble fragments (125 kDa and 165 kDa) by ADAM8, a member of the family of metalloprotease disintegrins (Naus et al., 2004). The ADAMs proteins (A Disintegrin And Metalloproteinase) belong to the zinc protease superfamily with essential physiological roles in fertilization, myogenesis, and neurogenesis. The functional ADAM metalloproteinases are involved in ‘‘ectodomain shedding’’ of receptors and adhesion molecules (Seals and Courtneidge, 2003). Soluble CHL1 processed by ADAM8 shows enhanced potential in stimulating neurite outgrowth and suppressing neuronal cell death *in vitro* (Naus et al., 2004).

The extracellular domain of CHL1 contains two different potential integrin-binding motifs. Integrins are cell surface receptors that interact with the extracellular

matrix (ECM) and mediate cell migration by transducing various signals from the outside to inside of the cells (Denda and Reichardt, 2007). The second Ig-like domain of CHL1 contains the RGD tripeptide sequence (Holm et al., 1996). This sequence was originally found within fibronectin and contributes to integrin binding. The RGD motif is also present in the extracellular domains of other L1 family members, such as L1, Ng-CAM (Neural-glia cell adhesion molecule), neurofascin. CHL1 also possesses another unique βI integrin binding motif DGEA within the sixth Ig-like domain as compared with other members of L1 family (Holm et al., 1996). It has been shown that CHL1 acts as a cooperative partner for β1 integrin in promoting cell migration (Buhusi et al., 2003). The linkage between CHL1 and the subcortical actin cytoskeleton, mediated by ankyrin, allows CHL1 to potentiate integrin-dependent cell migration toward extracellular matrix proteins (Buhusi et al., 2003).

The importance of CHL1 in neuron migration has been revealed by aberrant neurite orientation and delayed migration rate in cerebral cortex of CHL1 deficient (CHL1-/-) mice (Demyanenko et al., 2004). Migration of cortical neurons to their final location in the cerebral cortex is a fundamental process in the formation of the cerebral cortex. CHL1 mRNA is localized in a graded pattern in migrating neuronal precursors and enriched in layer V (Hillenbrand et al., 1999b). Cerebral cortex contains six different layers with characteristic distribution of neuronal cell types and connections (Shipp, 2007). During development, neurons migrate from the deeper layers, layer V and VI, to become the upper layers (Shipp, 2007). In contrast to the uniformly distributed L1, CHL1 is expressed in deep layer pyramidal neurons in a low-rostral to high-caudal gradient (Demyanenko et al., 2004). In the caudal (somatosensory and visual cortices) of CHL1-/- mice, a significant proportion (40%-60%) of deeper layer pyramidal neurons exhibit misoriented apical dendrites (Demyanenko et al., 2004).

In the rodents, the expression of CHL1 is not only restricted in neurons, but also

detectable in astrocytes, oligodendrocytes and Schwan cells (Hillenbrand et al., 1999a). In cerebellum, the localization of CHL1 is different from the other L1 family members. For example, L1 is abundantly expressed in unmyelinated and premyelinated axons of granule cells. Whereas, CHL1 is localized to apical radial fibers of polarized Bergmann glial (BG) cells, stellate interneurons and granule cells during the development of stellate axon arbors (Ango et al., 2008). In CHL1-/- mice, stellate axons deviate from BG fibers and show aberrant branching and orientation. Sequentially, the synapses formed between aberrant stellate axons and Pukinjie dendrites fail to be maintained (Ango et al., 2008). This study implicated an important functional feature of CHL1 at synapse. In cultured hippocampal neurons, CHL1 has been shown to localize at presynaptic terminals and plays a role in synaptic vesicle recycling by regulating uncoating of clathrin-coated synaptic vesicles in response to activation (Leshchyns'ka et al., 2006).

The *CHL1* gene in humans maps to chromosome region 3p26.1, which has been associated with intelligence and cognition (Angeloni et al., 1999a). Deletion of the *CHL1* gene in a patient with 3p-syndrome hints as a linkage between the *CHL1* locus and mental function (Angeloni et al., 1999a). 3p-sydrome is a rare disorder resulting from deletions within the distal end of chromosome 3p. The hallmarks of the syndrome include developmental delay, growth retardation (especially mental and psychomotor retardation), and craniofacial manifestations (Angeloni et al., 1999a). Investigation of mental retardation with 3p aberration led to evidence linking the translocation breakpoint in *CHL1 gene* to non-specific mental retardation. Moreover, a study using transgenic mice has shown that *CHL1 gene* alteration is connected to cognitive development and behavior in a gene dosage-dependent manner, suggesting *CHL1 gene* is a prime candidate for an autosomal form of mental retardation (Frints et al., 2003). Linkage analyses also suggested that CHL1 may be one of the susceptibility factor for schizophrenia (Sakurai et al., 2002; Chen et al., 2005; Lewis et al., 2003). Similar to

schizophrenia patients, CHL1-/- mice are impaired in prepulse inhibition (Irintchev et al., 2004), a measure for the ability of the central nervous system to gate the flow of sensory information (Van den et al., 2003). CHL1-/- mice also display alterations in emotional reactivity and motor coordination (Montag-Sallaz et al., 2003).

III.2 Cellular mechanisms implicated in CAMs-mediated neuronal migration and neurite outgrowth

Neurons possess the most complex and diverse shapes of all cell types. Neurons extend two types of neurites: axons and dendrites. Axons and dendrites are both functionally and morphologically distinct. Axons often travel long distances, making stereotypical turning decisions along their paths. Upon reaching their targets, axons produce terminal branches, and convert into presynaptic terminals. Unlike axons, dendrites usually do not extend over as long a distance away from the cell body, but often branch extensively, and give rise to dendritic trees (Goldberg, 2004; Fulga and Van Vactor, 2008). During brain development, CAMs have been shown to regulate neuronal migration and neurite outgrowth. They are not just adhesive molecules , but also function as signal transducing receptors at the cell surface (Maness and Schachner, 2007) .

The developing processes are led by a specialized end region known as the ‘‘growth cone’’ (Fig. III.2.). By interacting with guidance cues in the local environment, receptor molecules on the lamellipodia and/or filopodia trigger a cascade that ultimately leads to the assembly and/or disassembly of force-generating machinery within the growth cone (Dent and Gertler, 2003). Neuron migration on ECM protein substrates is enhanced by a functional interaction between CHL1 and βI integrin, since haptotactic migration of embryonic cortical neurons is inhibited in the presence of integrin-blocking antibodies *in vitro* (Buhusi et al., 2003). A trans-heterophilic interaction between

CHL1 and integrin may transduce signaling through pp60$^{c\text{-}src}$, PI3 kinase and ERK1/2 pathway in migrating cortical neurons responsible for correct laminar positioning (Buhusi et al., 2003; Schmid et al., 2004).

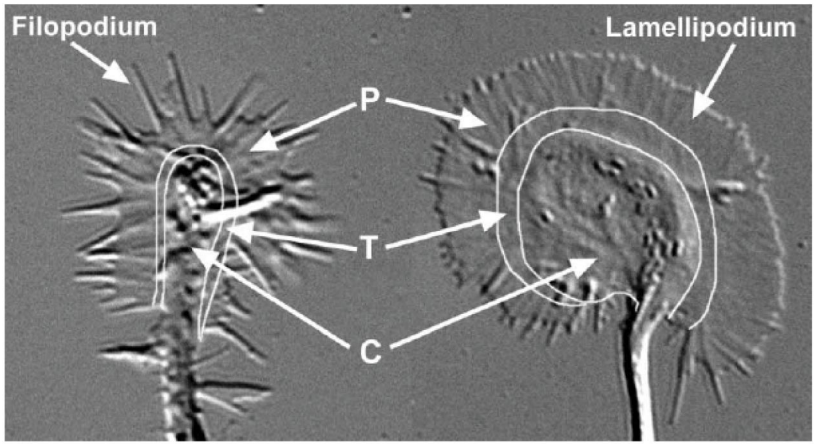

Figure III.2. Growth cones are composed of peripheral (P) domain, the transitional (T) domain and the central (C) domain. P domain includes finger-like filopodia and veil-like lamellipodia that exhibit amoeboid movement as the growing process explores its environment. T domain is a band of the growth cone at the interface of the P domain and the C domain. C domain is composed of thicker region invested by organelles and vesicles of varying sized (Dent and Gertler, 2003).

Growth cone movement also depends on the transport of membrane bound vesicles from the cell body to the growth cone and possible recycling of membrane vesicles via the process of endocytosis and membrane fusion within the growth cone itself. Receptor endocytosis seems to control semaphorin 3A (Sema 3A)-induced axon repulsion (Castellani et al., 2004). Sema 3A, a member of class-III semphorins, is a secreted protein that is involved in repulsive axon guidance and dendrite projection. Both CHL1 and L1 bind the Sema 3A receptor, Neuropilin-1 (NP-1), via a conserved sequence in the Ig1 domain, acts as obligate co-receptors to mediate Sema 3A-induced growth cone collapse and axon repulsion (Wright et al., 2007; Castellani et al., 2002). The term ‘‘growth cone collapse’’ describes the loss of lamellipodia and filopodia in response to a negative guidance cue. For example, following treatment with Sema 3A, sensory growth cones collapse and no longer exhibit protrusive activity (Fan et al., 1993). Sema3A promotes endocytosis of NP-1 during growth cone collapse and induces

co-internalization of L1 with NP-1 (Castellani et al., 2004). The effects of Sema 3A on growth cones collapse also coincide with depolymerization of actin filaments (Fan et al., 1993). The direct or indirect interaction between CHL1 and the ezrin-radixin-moesin (ERM) proteins in growth cones may modulate actin cytoskeletal rearrangement to facilitate Sema 3A-induced growth cone collapse (Schlatter et al., 2008).

Migration of newly born neurons is terminated upon their arrival at the targeted region and is followed by a period of neurite outgrowth. Neurite outgrowth is divided into three morphologically distinct stages termed protrusion, engorgement, and consolidation (Fig. III.3) (Goldberg and Burmeister, 1986). Protrusion occurs by the elongation of filopodia and lamellipodia (P domain, Fig. III.2), apparently through the polymerization of actin filaments. Engorgement occurs when the P domain become invested with vesicles and organelles from central domain (C domain) (Fig. III.2), like through Brownian motion and directed microtubule-based transport. Consolidation occurs as the proximal part of the growth cone assumes a cylindrical shape and transport of organelles becomes bidirectional, thus adding a new distal segment of axon (Dent and Gertler, 2003). These three stages give rise to the elongated neurites.

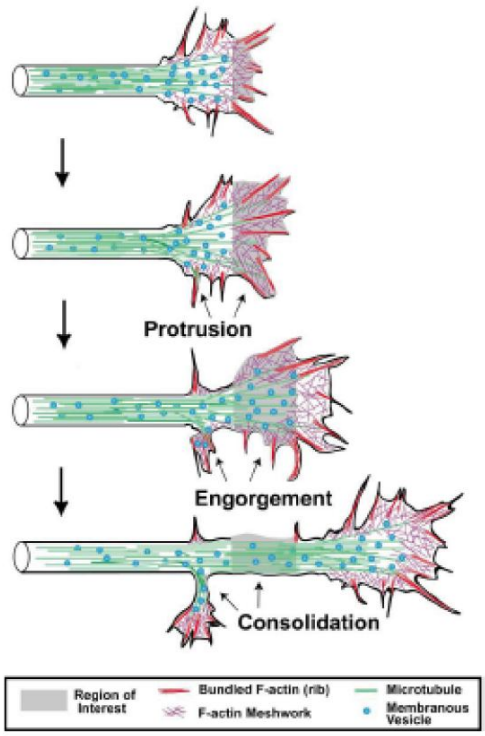

Figure III.3. Stages of neurite outgrowth formation. Neurite outgrowth contains three major stages: protrusion, engorgement, and consolidation (Dent and Gertler, 2003).

CAMs are capable of triggering intracellular signaling cascades to regulate neurite outgrowth. NCAM and L1 triggered signaling mechanisms with regard to neurite outgrowth coupled with the non-tyrosine kinase $p59^{fyn}$ and $pp60^{c\text{-}src}$. $P59^{fyn}$, but not $pp60^{c\text{-}src}$ is involved in NCAM-mediated signaling and neurite growth, whereas L1 signals through $pp60^{c\text{-}src}$ (Bodrikov et al., 2005; Loers et al., 2005). NCAM140 clustering actives $p59^{fyn}$ to induce recruitment and activation of focal adhesion kinase (FAK), followed by activation of the small GTP-binding protein c-Ras1. From c-Ras1, the signal progresses through sequential activation of serine/threonine kinase c-Raf-1 and MEK1/2, leading to phosphorylation of ERK1/2. L1 signaling joins the MAP kinase signaling pathway at the level of Raf. Thus, both molecules converge on this pathway, as shown by the fact that inhibition of FAK, Ras, Raf and MEK impair NCAM- and L1-dependent neurite outgrowth (Kiryushko et al., 2004). Interestingly, CHL1 has been related to both $p59^{fyn}$ and $pp60^{c\text{-}src}$ signaling for neuronal migration events (Buhusi et al., 2003;

Ye et al., 2008), but no evidence is present to prove that these two pathways are implicated in CHL1-mediated neurite outgrowth.

CHL1 engages the actin cytoskeleton through ERM proteins which bind to diverse CAMs including L1, ICAM (Inter-Cellular Adhesion Molecule), VCAMs (Vascular Cell Adhesion Molecule) and L-selectin, (Barreiro et al., 2002; Bretscher et al., 2002; Hamada et al., 2003; Ramesh, 2004; Schlatter et al., 2008). ERM proteins interact with these receptors through N-terminal FERM (Band 4.1, ERM) domain, while interact with filamentous (F)-actin through C-terminal domain (Ramesh, 2004). The intracellular domain of CHL1 contains a membrane-proximal RGGKY^{1112}SV sequence similar to an identified ERM interaction site in L1 (KGGKY^{1151}SV) (Cheng et al., 2005; Schlatter et al., 2008). In cultured cerebellar neurons, L1/ERM interaction has been shown to promote neurite outgrowth and branching on a L1 substrate (Cheng et al., 2005). Like L1, the recruitment of ERM to the plasma membrane by CHL1 is also required for CHL1-dependent neurite outgrowth and branching in cortical embryonic neurons (Schlatter et al., 2008).

Unlike L1 and NCAM which have strong potential to promote neurite outgrowth, CHL1 shows an ambiguous role on neurite outgrowth. Neurite outgrowth is known to be promoted when CHL1-Fc are coated as substrate (Hillenbrand et al., 1999b) . The promotion of neurite outgrowth may be due to the trans-interaction with a heterophilic receptor on neurons, probably β1 integrin (Buhusi et al., 2003). Because CHL1 could also promotes neurite outgrowth on a fibronectin substrate which then directly binds to integrin (Schlatter et al., 2008). Whereas, CHL1 -/- neurons show a more prominent neurite outgrowth on CHL1 substrate and a better recovery after spinal cord injury (Jakovcevski et al., 2007). A dual function hypothesis has been proposed for CHL1-dependent neurite outgrowth: CHL1 can promote neurite outgrowth by heterophilic interaction, but inhibit neurite outgrowth by homophilic interaction (Jakovcevski et al., 2007). The

specifc mechanism of CHL1 regulating neurite outgrowth is still unclear.

III.3 The role of lipid rafts in neurite outgrowth

Cells communicate and interact with the extracellular space through the plasma membrane that consists of a mosaic of proteins for receiving stimuli, for signaling in and out of the cells, and for interacting physically with the substrata. Microdomains in the plasma membrane, termed lipid rafts, are characterized as cold non-ionic detergent resistant extraction due to their enrichment in cholesterol and sphingolipids (Simons and Toomre, 2000). According to the lipid raft hypothesis, the plasma membrane is not just a continuous and homogenous fluid of lipids with proteins but inserted like a mosaic (Simons and Ikonen, 1997). Lipid rafts are thought to be involved in many cellular functions, in particular, signal transduction for extracellular stimuli (Golub et al., 2004).

For a growth cone to migrate and turn, spatial asymmetry of intracellular molecular information must be created. Therefore, spatial restricted recruitment and activation for signaling components govern important aspects of growth cone migration and navigation. Recent evidence indicates that membrane lipid rafts play an important part in growth cone migration and navigation. Several guidance receptors or receptor complex components associate with the lipid rafts (Marquardt et al., 2005; Yuan et al., 2005). NP-1, a Sema 3A receptor which interacts with both CHL1 and L1, produce downstream signaling for axon guidance in a cholesterol-sensitive manner (Guirland et al., 2004). CHL1 also associates with NB3, a glycosylphosphatidylinositol (GPI) anchored member of the contactin/F3 family of surface receptors (Ye et al., 2008). GPI-anchored molecules are enriched in lipid rafts (Sharma et al., 2004). The expression pattern of NB3 is similar to CHL1 which is exhibited in a low-rostral to high caudal gradient in the developing neocortex. Pyramidal neurons in NB3-deficient mice exhibit disoriented, often inverted, apical dendrites like in CHL1-deficient mice.

The interaction between CHL1 and NB3 enhances NB3 expression at the cell surface and activates protein tyrosine phosphatase α (PTPα), which in turn dephosphorylates and activates the src family kinase, $p59^{fyn}$ (Ye et al., 2008). Because $p59^{fyn}$ and NB3 are localized in raft membranes (Bodrikov et al., 2005; Sharma et al., 2004), CHL1 may play a role in regulating lipid raft-associated proteins which are important for neuronal projection in the developing caudal cortex.

Recycling of cell surface receptors by endocytosis and exocytosis within growth cones is critical for neurite outgrowth (Schmid et al., 2000; Pfenninger, 2009). Lipid rafts play an important regulatory role in this process (Kamiguchi, 2006). For example, L1 is internalized at the C-domain of growth cones and is recycled to the leading front (Kamiguchi and Lemmon, 2000b). The internalization of L1 is mediated by a clathrin-dependent pathway (Kamiguchi et al., 1998). The L1 cytoplasmic domain (L1 CD) carries the tyrosine endocytic motif recognized by the clathrin-associated adaptor protein, AP2 (Kamiguchi et al., 1998). Phosphorylation of this AP2-binding motif by raft-associated tyrosine kinase $pp60^{c\text{-}src}$ may regulate the endocytosis of L1 (Thelen et al., 2002; Simons and Toomre, 2000; Schmid et al., 2000). As the best characterized endocytic pathway, clathrin-mediated endocytosis is a ubiquitous process by which all types of eukaryotic cells internalize nutrients, antigens, growth factors, pathogens and recycling receptors (Jung and Haucke, 2007). However, lipid raft-associated proteins can be internalized through the pathway mediated by caveolae instead of clathrin coated vesicles (Mayor and Pagano, 2007). NCAM is endocytosed at the growth cone by both clathrin-dependent and caveolae-dependent pathway (Minana et al., 2001; Diestel et al., 2007). Since caveolin, a structure protein of caveolae, is less abundant in the brain (Lang et al., 1998), a distinct caveolae endocytic pathway mediated by flotillin/reggie has emerged recently (Mayor and Pagano, 2007). Flotillin/reggie, often used as a lipid raft marker expressed in a high level in the brain, is now considered to cooperate with various proteins

co-localized at the caveolae such as $p59^{fyn}$, contactin and amyloid precusor protein (APP) (Lang et al., 1998; Stuermer et al., 2001; Schneider et al., 2008). Deletion mutant of flotillin/reggie inhibits insulin-like growth factor (IGF)-induced neurite outgrowth in N2a neuroblasma cells, suggesting a role for flotillin/reggie in neurite outgrowth (Langhorst et al., 2008). However, whether the endocytosis of L1 molecules are mediated by the flotillin pathway is still little known. After endocytosis, some populations of the internalized membrane components are transported anterogradely along microtubes for reuse in the leading front (Kamiguchi and Lemmon, 2000a). This recycling process includes vesicle exocytosis that depends on interactions of soluble N-ethylamleimide-sensitive factor attachment protein receptor (SNARE) proteins, which are enriched in lipid rafts (Lin and Scheller, 2000). It has been shown that CHL1 is associated with SNARE complex in presynaptic terminal, and CHL1 deficient hippocampal neurons showed impaired vesicle recycling in response to high potassium stimulation (Aksana Andreyeva, 2008).

S-Palmitoylation increases the hydrophobicity of proteins and contributes to their association with lipid rafts microdomains. S-palmitoylation is the reversibly covalent attachment of fatty acids, such as palmitic acid, to cysteine residues of membrane proteins. Palmitoylation also appears to play an important role in subcellular trafficking of proteins between membrane compartments as well as in modulation of protein-protein interaction (Basu, 2004). The function of palmitoylation depends on the protein that is being considered. Palmitoylation of NCAM140 is necessary for its localization in lipid rafts, which is important for NCAM-dependent neurite outgrowth (Niethammer et al., 2002).

III.4 Calcium and neurite outgrowth

Calcium ions act as a second messenger inside the cell to mediate a wide spectrum of cellular function. During nervous system development, calcium ions

play a central role in the regulation of neurite growth and guidance (Henley and Poo, 2004).

The intracellular Ca^{2+}concentration regulated by many modulators, directly affects growth cone behavior, for example, increasing the rate of growth cone extension, turning growth cones and inducing growth cone collapse (Williams et al., 1992b; Kater and Mills, 1991). The voltage-dependent Ca^{2+} channels (VDCC) in growth cone induce Ca^{2+} influx to control the intracellular Ca^{2+}concentration. VDCCs are classified into several types based on their pharmacological and electrophysiological properties, such as L-type (L for large and long-lasting), T-type (T for tiny and transient) and N-type (N for neuronal) (Lacinova, 2005). Among them, L-type VDCC is considered to be most closely involved in growth cone activity by generating the long-lasting Ca^{2+} current (Zimprich and Bolsover, 1996; Ohbayashi et al., 1998). The differential effects of calcium on growth cone motility (e.g., growth and retraction) can be explained in part by the ‘‘set-point messenger’’ hypothesis (Kater and Mills, 1991). In this scheme, there is an optimal or set-point level of calcium that promotes maximal growth. Increasing calcium levels toward the set point will increase motility, whereas increasing it above the set-point decreases motility. Furthermore, both spatial and temporal changes in calcium concentration are likely to play essential roles in growth cone behavior (Doherty et al., 2000).

CAMs (e.g., NCAM, L1, N-cadherin) can drive neurite outgrowth by inducing calcium influx into neurons through both N- and L-type calcium channels (Williams et al., 1992a; Walsh and Doherty, 1997). However, there is no detectable increase in steady-state levels of calcium in the neuron when neurons are activated by L1 or soluble L1-Fc chimera (Harper et al., 1994; Archer et al., 1999). This paradox might be explained by the process of ‘‘calcium cycling’’, which balances calcium influx by rapid extrusion of calcium via membrane pumps. Any increase in calcium concentration would be restricted to the site of calcium

entry. The direct evidence has been showed by calcium imaging that CAM-stimulated neurite outgrowth is driven by localized submembrane increases in calcium concentration in growth cones, rather than global changes (Archer et al., 1999). The local nature of calcium provides a mechanism for localizing downstream signals (e.g., PKCβII and CaMKIIα) to a distinct region of a growth cone. A well-studied example is NCAM. Clustering of NCAM induces activation of PKCβII via fibroblast growth factor (FGF) receptor, and redistribution of the enzyme to lipid-rafts where PKC activates GAP-43, a cytoskeleton regulatory molecule (Leshchyns'ka et al., 2003). In addition, phosphorylation of GAP-43 results in the release of calmodulin (Skene, 1990). A combination of calcium influx and free calmodulin should serve to activate Ca^{2+}/calmodulin kinase. Furthermore, the association of NCAM with T- and L-type VDCC also brings calmodulin-dependent protein kinase IIα (CaMKIIα) into the locality of the Ca^{2+} influx in the neuronal growth cones (Bodrikov et al., 2008).

Turning of growth cone is caused by extension on one side and collapse on the other. In directional guidance of growth cone extension, spatially-restricted cytoplasmic Ca^{2+} signals mediate both attractive and repulsive responses of growth cones to several extracellular guidance cues. Recent studies indicate that different spatiotemporal patterns of Ca^{2+} signals trigger different motile behaviors of growth cones: a small local Ca^{2+} elevation triggers growth cone repulsion, whereas a modest local elevation induces growth cone attraction (Henley et al., 2004; Wen et al., 2004). However, relatively large local Ca^{2+} transients also cause growth cone repulsion (Robles et al., 2003). These findings suggest the existence of at lease three ranges of local Ca^{2+} signals involved in growth cone steering : small and large Ca^{2+} signals for repulsion and modest Ca^{2+} signals for attraction (Gomez and Zheng, 2006). This model is consistent the ‘‘set-point messenger’’ hypothesis (Kater and Mills, 1991; Kater et al., 1988). Therefore, Ca^{2+} signals, when present globally in the growth cones, can regulate overall growth cone motility and rate of extension, but, when locally elicited on one side

of the growth cone, can induce asymmetric growth cone motility that leads to steering of the growth cone.

Endocytic recycling of the membrane is Ca^{2+} dependent, providing a mechanism by which Ca^{2+} signaling may regulate cell migration and growth through the modulation of substrate adhesion. In the same time, adhesion may also provide feedback regulation of Ca^{2+} signals in the cell. A recent study showed that localized Ca^{2+} signals induce asymmetric exocytosis to result in a turning response (Tojima 2007).

III.5 Spectrin mesh-work and its functions in nervous system

Spectrin is now recognized as a ubiquitous scaffolding protein that acts in conjunction with a variety of adaptor proteins to organize membrane micro-domains on both the plasma membrane as well as intracellular organelles.

The spectrin cytoskeleton is a two-dimensional submembrane protein meshwork. Alpha and beta subunits assembled anti-parallel and side-to-side to form heterodimers. Alpha/beta heterodimers, in turn, form end-to-end tetramers in which the N-terminus of each alpha subunit associates with the C-terminus of each beta subunit. In human erythrocytes, five of the six spectrin tetramers are linked by one short actin filament (Bennett and Baines, 2001). A defining feature of spectrin is the presence of many tandem, anti-parallel coiled-coil repeats (Yan et al., 1993). Each spectrin repeat is composed of three helices (A, B and C). Conformational rearrangements involving the helix B-C loop, variations in the length of the B helix and variations in the degree of super coiling appear to control both the flexibility of the link and the overall length of the molecule (Grum et al., 1999).

Currently characterized spectrins in human include two alpha-subunits (α1, α2) and five beta-subunits (β1, β2, β3, β4, β5/β-H) (Bennett and Baines, 2001).

Combinatorial association of alpha-spectrins with various beta-spectrin subunits yields alpha/beta heterotetramers with distinct functions and patterns of expression. Alpha-spectrins contain 22 domains with the following features: domains 1-9 and 11-21 are spectrin repeats; domain 10 is an SH3 (src homology 3) domain; the COOH-terminal domain 22 is related to calmodulin (Dubreuil et al., 1989). Beta-spectrins contain 19 domains beginning with a highly conserved NH_2-terminal actin-binding domain, followed by 17 consecutive spectrin repeats and ending with a COOH-terminal domain which includes a pleckstrin-homology (PH) domain (Bennett and Healy, 2008) (Fig. III.4).

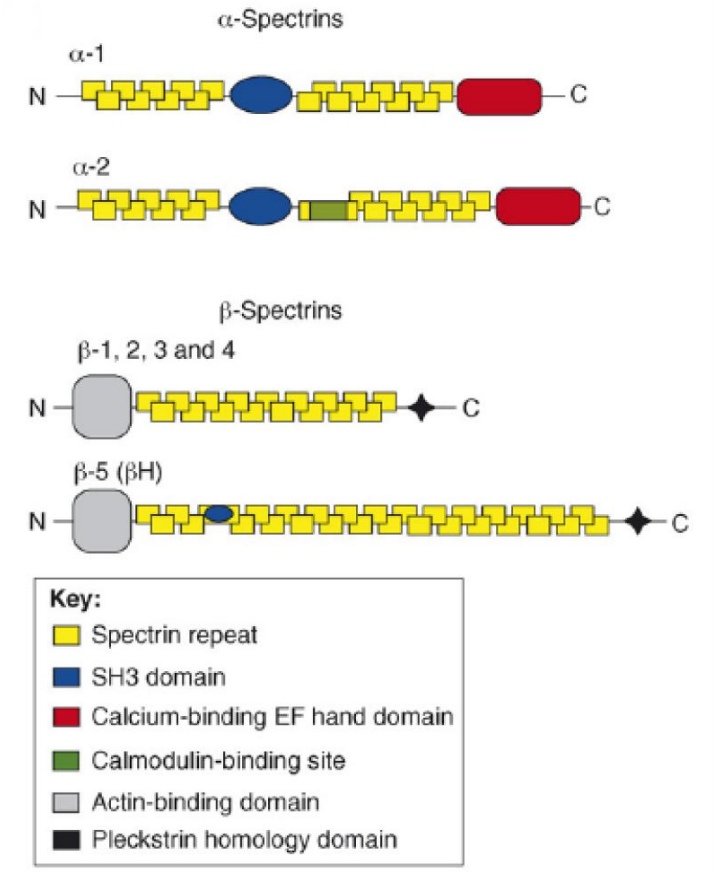

Figure III.4. Schematic structures of spectrins. Spectrins comprise modular units called spectrin repeats. α spectrins are featured by Src-homology (SH) domain and EF-hand domain (a protein fold associated with calcium-binding activity). NH2-terminal of β spectrin contains the actin-binding domain. The pleckstrin-homology domain promotes β spectrin associated with the plasma membrane (Bennett and Healy, 2008).

As a major adapter protein, ankyrins connect integral membrane proteins with spectrin meshwork. The ankyrin gene family of mammals currently includes three members: ankyrin-R (R for restricted), first characterized in erythrocytes;

ankyrin-B (B for broadly expressed), first characterized in brain; and ankyrin G (G for general or giant), independently discovered in searches for components of node of Ranvier and for epithelial ankyrins (Bennett and Baines, 2001). Ankyrins are modular proteins comprised of three domains conserved among family members as well as specialized domains found in alternatively spliced isoforms. Ankyrin contains a conserved NH_2-terminal membrane-binding domain, a spectrin-binding domain, a death domain and a regulatory domain (Bennett and Healy, 2008) (Fig. III.5). The membrane binding domain is comprised of 24 copies of a 33 residue repeat known as the ANK repeat that is involved in protein recognition in many types of proteins (Sedgwick and Smerdon, 1999). The ANK repeat stack behaves like a reversible spring when it is stretched by atomic force microscopy (Lee et al., 2006). The spectrin-binding domain allows ankyrins to coordinate integral membrane proteins with spectrin. The death domain is the most highly conserved domain whose function is unknown. The regulatory domain is the most variable region of ankyrins and regulates the affinity between ankyrin and its binding partners (Bennett and Healy, 2008).

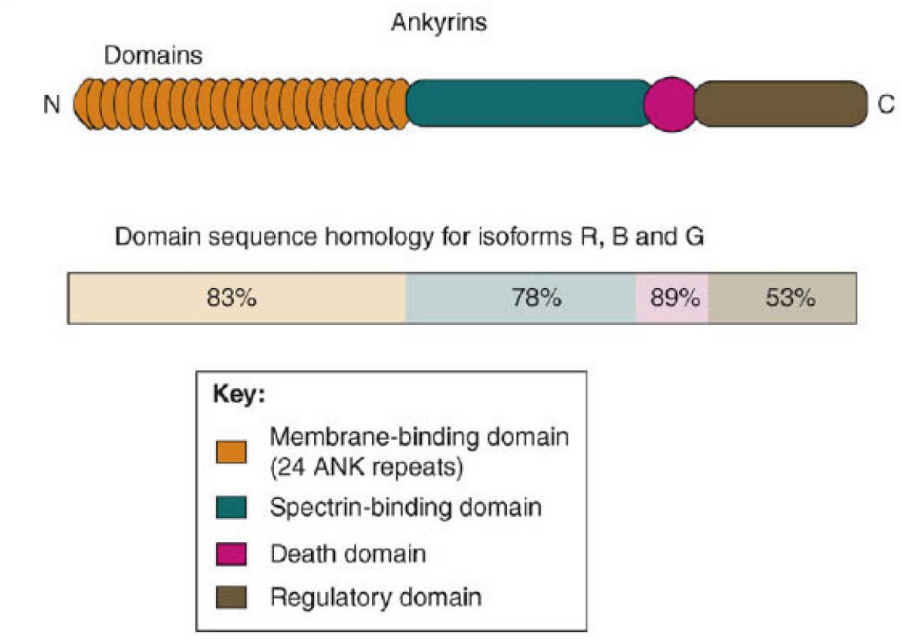

Figure III.5. Domain structure of ankyrins. Ankyrin contains three isoforms: ankyrin-R, ankyrin-B and

ankyrin-G. The membrane-binding domain of ankyrin comprises 24 ANK repeats which binds to many integral membrane proteins. The spectrin-binding domain allows ankyrin to coordinate membrane proteins with spectrin. The death domain is highly conserved, but the function is unknown. The regulatory domain is the most variable region of ankyrins and regulates the affinity between ankyrin and its binding partners (Bennett and Healy, 2008).

In the L1 family, the cytoplasmic domain of L1 molecules contains a conserved sequence (FIGQ/AY) that reversibly binds to ankyrin, which couples L1 to the subcortical spectrin mesh-work. Separate subdomains within ankyrin recruit L1 molecules, ion channels and pumps to associate with the spectrin meshwork. L1 binding to ankyrin is regulated by phosphorylation of the FIGQY tyrosine. This modification, which decreases ankyrin binding, occurs during axon growth and migration in the developing cortex, whereas dephosphorylation, which promotes ankyrin binding, increases during synaptic targeting (Davis and Bennett, 1993; Jenkins et al., 2001).

The association between CAMs and spectrin is important for CAM-dependent functions. Unlike L1, NCAM directly interacts with spectrinβ1. Transmembrane NCAM isoforms interact directly with spectrin both in lipid rafts and in raft-free membrane, whereas NCAM120 interacts with spectrin in rafts. Neural migration and neurite outgrowth rely on the rearrangement of cytoskeletal elements. Spectrin serves as a platform for the association of NCAM140 with the receptor-like protein tyrosine phosphatase RPTPα, a known binding partner and activator of $p59^{fyn}$, important for neurite outgrowth. PKCβ2 forms a detergent-insoluble complex with NCAM140/NCAM180 through spectrin, which is necessary for NCAM-mediated neurite outgrowth.

The importance of spectrin in neurite morphological change was first demonstrated by microinjection of anti-β-spectrin antibodies in cultured NB2a neuroblastoma cells which inhibited the extension of neurites (Sihag RK, 1996 J Neurosci res 44(5) 430-7). More recent evidence suggests that spectrin plays a more essential role in maintaining axon integrity instead of promoting axon

outgrowth in the nematode *Caenorhabditis elegans*, whose β-spectrin is encoded by a single gene, unc-70. Unc-70 mutants exhibit abnormal axon morphology, such as truncated processes, spontaneous breaks, and elaborate branching in neuronal process (Hammarlund et al., 2000; Hammarlund et al., 2007). Axons in β-spectrin mutants spontaneously break. After breaking, the neuron attempts to regenerate by initiating a new growth cone but this second round of axon extension is error prone compared with initial outgrowth. Considering that spectrin-based membrane skeleton is required for membrane integrity in erythrocytes, Hammarlund, M. *et al.* hypothesize that the spectrin scaffold provides the possibility for the long and thin axon extensions in response of external forces during development. Brain spectrin was detected throughout the neuron, extending into growth cones by immunostaining, whereas the spectrin cleaved by calpain is limited to the consolidated region in neurites, which creates a sharp boundary between the neurite shaft and the growth cone (Meur, A.M 2009). During development, a stable neurite shaft following dynamic growth cone is considered to be consolidated. Consolidation results from the collapse of the proximal part of the growth cone and the suppression of protrusive activity along the neurite (Luo 2002, Dent and Gertler 2003). Calpain protease activity localized to the neurite shaft is essential for the consolidation of neurite shaft against branching activity. Proteolysis of spectrin by calpain probably induces a local disconnection of actin filaments from the plasma membrane (Hu and Bennet, 1991). Another interesting feature for spectrin meshwork is implicated in axon guidance. Bata-spectrin is required in neurons for proper midline axon guidance in the Drosophila embryonic central nervous system. In beta-spectrin mutants many axons inappropriately cross the CNS midline, suggesting a role for beta-spectrin in midline repulsion (Garbe et al., 2007).

In the pre-synapse, spectrin is important for neurotransmitter release and synapse stabilization. Brain spectrin (αSpIIΣ1/βSpIIΣ1) is distributed primarily in axons and presynaptic terminals and brain spectrin (αSpIΣ1/βSpIΣ2) is located in

the soma, dendrites and postsynaptic terminals (Zagon et al., 1986a). In the presynaptic terminal, nonerythroid spectrin (αSpIIΣ1/βSpIIΣ1) with small synaptic vesicles in the presynaptic terminal (Zagon et al., 1986a). Small spherical synaptic vesicles are tethered to the active zone of the presynaptic plasma membrane by fibers of nonerythroid spectrins (Landis et al., 1988). βSpIIΣ1 contains a synapsin-binding domain capable of interacting with synapsin and small synaptic vesicles (Zimmer et al., 2000). Injection of specific antibodies directed against epitopes within the synapsin binding domain into presynaptic neuron could specifically block synaptic neurotransmission (Sikorski et al., 2000). Presynaptic spectrin is also essential for synapse stabilization. Pielage *et al.* use transgenic dsRNA to selectively eliminate spectrin protein during postembryonic development. They demonstrate that lack of presynaptic spectrin in Drosophila neuromuscular junction leads to synapse disassembly and elimination. In addition, loss of presynaptic spectrin leads to the disorganization of several synaptic cell adhesion molecules (Pielage et al., 2005).

Recycling of cell surface receptor is important for axon growth, guidance and synaptic plasticity, whereas as a major membrane cytoskeleton component in the brain, the function of spectrin in vesicle recycling is largely unclear (Dent and Gertler, 2003; Kamiguchi, 2006; Jung and Haucke, 2007; Zagon et al., 1986b). Most of the studies about the involvement of spectrin in vesicle recycling focus on non-neuronal cells. In erythrocytes, endocytosis is preceded by the formation of spectrin-free zones at sites of membrane budding (Hardy et al., 1979). In the clathrin-mediated endocytic pathway, dissociation of the clathrin lattice from the spectrin membrane cytoskeleton is necessary for the final stage of budding. The removal of spectrin may be mediated by the proteolytic action of calpain I (Harris and Morrow, 1990). An in vitro study has shown that limited proteolysis by calpain promoted dissociation of spectrin from the membrane (Hu and Bennett, 1991). Besides being considered simply as a barrier for endocytosis, spectrin may play a functional role in vesicle recycling. Spectrin is necessary for the maintenance of

endosomes in the epithelia of Drosophila, suggesting that this molecule is required for sorting decisions at the early endosome (Phillips and Thomas, 2006).

IV Materials

IV.1 Mouse strains

In this study 1-3-day-old wild type (CHL1+/+) and CHL1 deficient (CHL1-/-) mice (Montag-Sallaz et al., 2002) were used. CHL1-/- mice were back-crossed into a C57BL/6J genetic background. The genotype of mutant and wild type mice was determined using polymerase chain reaction (PCR) with template DNA isolated from tail biopsies.

IV.2 Buffers and solutions

Bi-distilled water (ddH_2O) was used for the preparation of all buffers and solutions.

Name	Composition
Blocking buffer (for Western-blot analysis)	5 % (w/v) skimmed milk powder (Frema Reform) in TBS
DNA sample buffer (5x) (for DNA agarose gels)	20 % (v/v) glycerol in 1x TAE 0.025 % (w/v) Orange G
Destaining solution (for coomassie blue staining)	45% methanol 10% acetic acid
Elution buffer (for production of recombinant proteins)	20 mM reduced glutathione 50 mM Tris-HCl pH 8.0
Ethidium bromide staining	10 µg/ml ethidium bromide in 1x TAE

solution	(0.025 mM in 1x TAE)
(for DNA agarose gels)	
Homogenization buffer	0.32 M sucrose
(for brain homogenization and membrane fraction isolation)	5 mM Tris-HCl, 1 mM $MgCl_2$ 1 mM $CaCl_2$ 1 mM $NaHCO_3$ pH 7.4
Homogenization buffer	0.32 M sucrose
(for growth cone fraction isolation)	1 mM $MgCl_2$ 5 mM Tris-HCl, pH 7.4
IPTG stock solution (1M)	238 mg/ml in ddH_2O
(for production of recombinant proteins)	
Lysis buffer	1x PBS
(for production of recombinant proteins)	1% Triton X-100 1x complete^{TM} EDTA-free protease inhibitor cocktail pH 7.4
Precipitation buffer	136 mM NaCl

(for cell surface biotinylation)	10 mM Na_2HPO_4
	2.7 mM KCl
	1.8 mM KH_2PO_4
	5 mM EGTA
	5mM EDTA
	pH 7.4
PHEM buffer	60 mM PIPES
(for detergent fraction of spectrin)	25 mM HEPES
	10 mM EGTA
	2 mM $MgCl_2$
	pH 6.9
Phosphate buffered saline (PBS)	136 mM NaCl
	10 mM Na_2HPO_4
	2.7 mM KCl
	1.8 mM KH_2PO_4
	pH 7.4
Phosphate buffered saline/Mg/Ca	136 mM NaCl
(PBS/MC)	10 mM Na_2HPO_4
(for cell surface biotinylation)	2.7 mM KCl
	1.8 mM KH_2PO_4
	pH 7.4
	1mM $CaCl_2$

	0.5 mM $MgCl_2$
Phosphate buffered saline/Tween (PBST) (for ELISA and cell surface biotinylation*)*	PBS 0.1 % (v/v) Tween 20
Radio immunoprecipitation assay (RIPA) buffer (for co-immunoprecipitation)	50 mM Tris-HCl, pH 7.5 150 mM NaCl 10 mM KCl 1 mM $Na_4P_2O_7$ 1 mM NaF 2 mM Na_3VO_4 1 % (v/v) NP-40 1 mM PMSF (2 mM EGTA)
SDS-PAGE running buffer (for SDS-PAGE)	25 mM Tris 200 mM glycine 0.1 % (w/v) SDS
SDS sample buffer (5x) (for SDS-PAGE)	310 mM Tris-HCl, pH 6.8 25 % (v/v) glycerol 10 % (w/v) SDS 4.5 % (v/v) β-mercaptoethanol 0.015 % (w/v) bromphenol blue

Separating gel	375 mM Tris-HCl, pH 8.8
(for SDS-PAGE)	0.1 % (w/v) SDS
	0.02 % (w/v) APS
	0.1 % (v/v) TEMED
	8% (w/v) Acrylamide/Bis solution (29:1)
Stacking gel	125 mM Tris-HCl, pH 6.8
(for SDS-PAGE)	0.13 % (w/v) SDS
	0.05 % (w/v) APS
	0.2 % (w/v) TEMED
	4% (w/v) Acrylamide/Bis solution (29:1)
Staining solution	1% coomassie blue R-250
(for coomassie blue staining)	45% methanol
	10% acetic acid
Stripping buffer	25 mM glycine-HCl, pH 2.2
(for Western-blot analysis)	1 % (w/v) SDS
Sucrose, 0.75 M	0.75 M sucrose
(for growth cone fraction isolation)	1 mM $MgCl_2$
	5 mM Tris-HCl, pH 7.4
Sucrose, 1.0 M	1 M sucrose
(for growth cone fraction isolation)	1 mM $MgCl_2$
	5 mM Tris-HCl, pH 7.4

80 % Sucrose stock solution in ddH_2O (for growth cone isolation)	80 % (w/v) sucrose in ddH_2O
80 % Sucrose stock solution in Na_2CO_3 (for lipid raft isolation)	80 % (w/v) sucrose in 0.2 M Na_2CO_3
10 % Sucrose in TBS (for lipid raft isolation)	10 % (v/v) sucrose (from sucrose stock in Na_2CO_3) in TBS
30 % Sucrose in TBS (for lipid raft isolation)	30 % (v/v) sucrose (from sucrose stock in Na_2CO_3) in TBS
1 % Triton X-100 (for lipid raft isolation)	1 % (v/v) Triton X-100 (Sigma-Aldrich) in TBS
Tris buffered saline (TBS) (for Western-blot analysis)	50 mM Tris-HCl, pH 7.4 150 mM NaCl
Tris buffer saline /tween (TBS-T) (for Wester-blot analysis)	50 mM Tris-HCl, pH 7.4 150 mM NaCl 0.1 % (v/v) Tween 20
Tris acetate EDTA (TAE) buffer (50x) (for DNA agarose gels*)*	2 M Tris-acetate, pH8.0 100 mM EDTA
Wash buffer (for production of recombinant proteins)	1x PBS 1% Triton X-100

pH 7.4

IV.3 Primary antibodies

Name	Description and working condition
Anti-Actin	Rabbit polyclonal antibody (Sigma-Aldrich), raised against a synthetic actin N-terminal peptide, Immunoblotting 1:1000 in blocking buffer.
Anti-Ankyrin B	Mouse IgG1 monoclonal antibody, (BD Transduction Laboratories), raised against the human ankyrin B spectrin-binding domain, immunobloting 1:1000 in blocking buffer.
Anti-α_A adaptin (AP2)	Mouse IgG1 monoclonal antibody, (BD Transduction Laboratories), raised against amino acids 38-215 of the mouse α_A adaptin, immunobloting 1:1000 in blocking buffer.
Anti- βI spectrin	Goat polyclonal antibody (Santa cruz Biotechnology), raised against a peptide mapping at the C-terminus of the human βI spectrin, immunobloting 1:1000 in blocking buffer.
Anti- βII spectrin	Mouse IgG1 monoclonal antibody (BD Transduction Laboratories), raised against amino acids 2101-2189 of the human βII spectrin, immunoblotting 1:1000 in blocking buffer.

Anti-βIIIspectrin	Goat polyclonal antibody (Santa Cruz Biotechnology.), raised against a peptide mapping near the C-terminus of the human βIII spectrin, immuniblotting 1:1000 in blocking buffer.
Anti-Clathrin	Mouse IgG1 monoclonal antibody (BD Transduction Laboratories), raised against amino acids 4-171 of rat clathrin heavy chain, immunoblotting 1:2000 in blocking buffer.
Anti-CHL1	Rabbit polyclonal antibody, produced in the lab of Prof. Schachner, raised against the extracellular domain of the mouse CHL1 (Rolf et al., 2003), immunoblotting 1:1000 in blocking buffer.
Anti-Contactin/F3	Goat polyclonal antibody (R&D System), raised against the recombinant human contactin-1, immunoblotting 1:500 in blocking buffer.
Anti-Flotillin-1	Mouse IgG1 monoclonal antibody (BD Transduction Laboratories), raised against amino acids 312-428 of the mouse flotillin-1, immunoblotting 1:1000 in blocking buffer.
Anti-GAPDH	Mouse monoclonal antibody (Chemicon), raised against GAPDH from the rabbit muscle, immunoblotting 1:2000 in blocking buffer.
Anti-GST	Mouse monoclonal antibody (Novagen), raised against GST, ELISA assay 1: 10,000 in 3% BSA in PBS-T.
Anti-$p59^{fyn}$	Rabbit polyclonal antibody (Santa Cruz Biotechnology), raised against the N-terminal of the human $p59^{fyn}$,

	immunoblotting 1:1000 in blocking buffer.
IgG, rabbit	IgG from rabbit serum (Sigma-Aldrich)
IgG, rat	IgG from rat serum (Sigma-Aldrich)

IV.4 Secondary antibodies

Secondary antibodies were purchased from Jackson ImmunoResearch Laboratories. The antibodies were coupled to horseradish peroxidase (HRP) and purified by immunoaffinity chromatography. To analyze immunoblots of co-immunoprecipitation assays, preabsorbed antibodies were used to minimize cross-reactions to serum proteins of other species. The antibodies were used in dilutions of 1:20,000 or 1:50,000 in blocking buffer.

IV.5 DNA and protein standards

DNA/protein standards are used to indicate the molecular weight for electrophoresis.

Name	Company
1 kb DNA Ladder	Invitrogen
Precision Plus Protein™ All Blue Standards (10 bands of 10-250 kDa, prestained in blue)	Bio-Rad Laboratories
Precision Plus Protein™ Dual Color Standards (10 bands of 10-250 kDa, prestained in blue and red)	Bio-Rad Laboratories

IV.6 Bacterial strains and mammalian cell lines

Bacterial strains were made chemically competent for transformation with plasmid DNA.

Name	Description	Company
Escherichia coli DH5α	F- φ80dlacZ⊿M15 ⊿(lacZYA-argF)U169 deoR recA1 endA1 hsdR17(rk--,mk+) phoA supE44 λ- thi-1 gyrA96 relA1	New England Biolabs
Escherichia coli TOP 10 cells	F- mcrA D(mrr-hsdRMS-mcrBC) f80lacZDM15 DlacX74 deoR recA1 araD139 D(ara-leu)7697 galU galK rpsL (StrR) endA1 nupG	Invitrogen
Escherichia coli BL-21	F-, ompT, hsdSB (rB-, mB-), dcm, gal, λ(DE3), pLysS, Cmr	Novagen
Flp-InTM-3T3 cells	The 3T3 fibroblast cell line originally obtained from Swiss mouse embryo tissues. The Flp-In host cell line stably expresses the lacZ-ZeocinTM fusion gene.	Invitrogen

IV.7 Bacterial media

Bacterial media were autoclaved and supplemented with antibiotics prior to use.

Name	Composition
LB-medium	10 g/l bacto-tryptone, pH 7.4
	10 g/l NaCl 5 g/l yeast extract
	Antibiotic: 100 mg/l ampicillin
LB-agar	20 g/l agar in LB-medium
	Antibiotic: 100 mg/l ampicillin

IV.8 Plasmids

The pEF/FRT/V5 Directional TOPO Expression Kit was purchased from Invitrogen GmbH and used for full-length CHL1 subcloning.

IV.9 Cell culture media and material

Sterile polystyrene cell culture plates and flasks heavy metal-free, non-pyrogenic and non-cytotoxic were purchased from Greiner Bio-One GmbH.

NIH 3T3 cell culture medium and solutions

Name	Composition
HBSS	Without Ca^{2+} and Mg^{2+}, with phenol red (PAA Laboratories)
Trypsin/EDTA (1:250)	0.5 mg/ml trypsin, 0.22 mg/ml EDTA, without Ca2+ and Mg2+ (PAA Laboratories)

NIH 3T3 cell growth medium	(DMEM/F-12) without L-glutamine (Invitrogen GmbH), supplemented with: 10 % (v/v) donor calf serum (DCS) (Invitrogen) and 2mM L-glutamine (PAA Laboratories)
NIH 3T3 cell freezing medium	cell growth medium supplemented with: 20 % (v/v) donor calf serum (DCS) (Invitrogen) and 10 % (v/v) DMSO (Fluka)

Primary cell culture medium and solutions

Name	Composition
Growth medium (hippocampal neurons)	Neurobasal™-A medium (Invitrogen) Supplemented with: 1x B-27 (Invitrogen), 2 mM GlutaMAX™ (Invitrogen), 2 ng/ml basic FGF (R&D Systems)
Dissection solution (hippocampal neurons)	Neurobasal™-A medium (Invitrogen) Supplemented with: 1x B-27 (Invitrogen), 2 mM GlutaMAX™ (Invitrogen)
Digestion solution (hippocampal neurons)	Neurobasal™-A medium (Invitrogen) Supplemented with: 0.2 mg/ml DNase I (Sigma-Aldrich), 2 mg/ml Papain (Sigma-Aldrich)
Dissociation solution (hippocampal neurons)	Neurobasal™-A medium (Invitrogen) Supplemented with: 1x B-27 supplement (Invitrogen GmbH), 0.2 mg/ml DNase I (Sigma-Aldrich)
Fixing solution (10x)	4 % (v/v) PFA in PBS

IV.10 Inhibitors

Lipid biosynthesis inhibitors used for the neurite outgrowth assay, such as mevinolin, *N*-butyldeoxynojirimycin (NB-DNJ), and fumonisin B are purchased from Sigma-Aldrich.

Inhibitors used for blocking VDCC are purchased from Alomone Laboratories: nifidipine for L-type VDCC, pimozidie for T-type VDCC.

IV.11 Centrifuges

Name	Company
Beckman Optima XL-80 Ultracentrifuge with SW32Ti, SW40Ti, SW55Ti and SW80Ti rotors	Beckman
Eppendorf Centrifuge 5804 R	Eppendorf
Eppendorf Centrifuge 5810 R	Eppendorf
Sorvall RC50*plus* centrifuge with SLA3000, SLA 1500, SA600 and HB-6 rotors	Kendro

V METHODS

V.1 Molecular biological methods

V.1.1 Molecular cloning

To generate the expression constructs encoding full length CHL1, we use the pEF/FRT/V5-D-TOPO cloning kit, which designed to facilitate rapid, directional cloning and expression of PCR products using the Flp-In System from Invitrogen. When co-transfected with the pOG44 Flp recombinase expression plasmid into Flp-In mammalian host cell line, the pEF/FRT/V5-D-TOPO vector containing the PCR product of interest is integrated in a Flp recombinase-dependent manner into the genome.

V.1.1.1 PCR reactions

Primers designed according to the GenBank DNA sequence for CHL1 published in GenBank (accession no. NM_007697.2) were used to PCR amplify full-length CHL1 using plasmid DNA containing full-length murine CHL1 in pcDNA3 as a template and the Phusion High-Fidelity PCR Kit (BioLabs).

Primers:

Name	DNA sequence
Forward primer:	5'-CACCATGATGGAATTGCCATTATGTGGAAGAGGAC-3'
Reverse primer:	5'-TCATGCCCGGAGTGGGAAGGTG-3'

The reaction mixture using Phusion High-Fidelity PCR Kit (BioLabs)

Component	Amount per reaction
H_2O	34 µl
5xphusion HF Buffer	10µl
10 mM dNTPs	1µl
10 pM primer forward primer	1µl
10 pM primer reverse primer	1µl
10 ng/µl template DNA	1µl
DMSO	1.5µl
phusionDNA polymerase	0.5 µl

PCR programme

Cycles	Temperature	Time
1	98°C	30 sec
36	98°C	10 sec
	63°C	20 sec
	72°C	2 min
1	72°C	10 min

V.1.1.2 TOPO cloning reaction

The TOPO cloning reaction was used to join the PCR product with the pEF5/FRT/V5/-D-TOPO® vector.

Reaction mixture

Reagents	Amount
Fresh PCR product	0.5-4 µl
Salt Solution	1µl
Sterile Water	add to a final volume of 5µl
TOPO vector	15µl
Final volume	6µl

The reaction mixture was gently mixed and incubated for 5 min at room temperature, then place on ice. Until used for bacterial transformation.

V.1.2 Chemical transformation of bacteria

100 µl of competent cells (*E. coli*) were mixed with 50-100 ng of plasmid DNA and incubated on ice for 10 min. The cells were then heat shocked (42°C for 50 s), chillied on ice for 2 min and growth at 37°C in 450 µl of LB medium in a shaker incubator for 45 min. Finally, 50 µl of transformed bacteria was plated on LB agar plates containing the appropriate antibiotic.

V.1.3 Purification of plasmid DNA

V.1.3.1 Small scale plasmid DNA purification

3 ml of LB medium containing appropriate selective antibiotic (100 µg/ml ampicillin) was inoculated with a single colony and incubated overnight at 37°C with vigorous shaking (220 rpm). Bacteria were harvested by centrifugation at 12, 000 g for 1 min at room temperature. Plasmid DNA was isolated according

to the manufacturer instructions (Invitrogen) and eluted by 70 µl of nuclease free water (Amion).

V.1.3.2 Large scale plasmid DNA purification

This method is designed for purification of up to 500 µg of endotoxin-free plasmid DNA. 3 ml of starter bacterial culture was incubated with a single bacterial colony from freshly streaked selective agar plates. The inoculation was performed in LB medium with appropriate selective antibiotic. The starter culture was then incubated at 37°C for approximately 8 h with vigorous shaking. Then the starter culture was diluted 1:1000 into selective LB medium and incubated overnight with vigorous shaking at 37°C. The bacteria were harvested by centrifugation at 6000 g for 15 min and DNA isolated using an Endofree Plasmid Maxi Kit (Qiagen) and dissolved in nuclease-free water (Amion).

V.1.4 Restriction digestion of DNA

To verify the isolated recombinant plasmids, DNA was digested into different fragments by restriction enzymes. All digestions were performed using restriction enzyme in accordance with the New England Biolabs catalogue and relevant technical references.

V.1.5 Horizontal agarose gel electrophoresis of DNA

DNA purity was determined using horizontal agarose-gel electrophoresis. Briefly, 1% (w/v) agrose gels were prepared in 1xTAE buffer. Digested DNA was then separated using a Bio-Rad electrophoretic chamber and TAE buffer at the constant votage (90 V) for 50 min. DNA-sample buffer was added to the DNA samples, prior to loading on the gel. To visualized the DNA, gels were incubated with 0.5 µg/ml ethidium bromide in TAE buffer and scanned using an

E.A.S.Y. UV-light documentation system (Herolab, Wiesloh).

V.1.6 Determination of DNA concentration

DNA concentration was evaluated using a calibration curve and BioSpec-mini spectrometer (Shimadzu). DNA absorbance was measured at 260nm. An A260/A280 ratio was used to estimate the purity of DNA because proteins absorb at a wave length of 280 nm. The ratio of DNA absorbance at 260 nm and 230 nm was also measured to ascertain contamination by carbohydrates, phenols, peptides and aromatic compounds that absorb at a wave length of 230 nm.

V.1.7 Sequencing of DNA

DNA sequencing was performed by the ZMNH, Hamburg sequencing facility. Using 1 µg of DNA diluted in 7 µl ddH2O along with appropriate sequencing primers (10 pM).

V.1.8 Site directed mutagenesis

Full-length CHL1 cloned in pEF5/FRT/V5/-D-TOPO® vector was used as template. Single amino acid changes were made using QuikChange® II XL Site-Directed Mutagenesis Kit from Stratagene as per the manufacturer's protocol. The following primers were used to generate the C1102S mutation within the CHL1 intracelluar domain.

Name	DNA sequence
Forward primer:	5'-ACACTGATATTGTTAACTATTTGCTTTGTGAAGAGGAACAG AGGT-3'

Reverse primer:	5'-ACACTGATATTGTTAACTATTTCCTTTGTGAAGAGGAACAG AGGT-3'

V.2 Protein biochemical methods

V.2.1 Production of recombinant proteins

V.2.1.1 Expression of N-terminally GST-taged recombinant proteins in *E.coli*

BL21 protease-deficient bacteria were transformed with pGEX-4T-2 expression vectors (Amersham Pharmacia Biotech) encoding the intracellular domain of CHL1/L1 and then grown overnight on ampicillin-containing LB plates. A single colony was inoculated into 20 ml of LB medium containing 100 µg/ml ampicillin and incubated overnight at 37 °C with constant shaking. The non-induced onvernight culture was transferred into a 1 liter expression culture (1:50) and incubated at 37 °C under vigorous shaking until the culture reached an optinal density (OD_{600}) of 0.6. Protein expression from large scale preparation was induced by 1mM IPTG. The protein expression was controlled by collecting small aliquots of the culture after IPTG induction every hour. After 4h of growth at 37 °C, cells were harvested at 4,000 g for 20 min at 4 °C.

V.2.1.2 Bacteria lysis and French press

Harvested cells were resuspended throughly in lysis buffer, transferred to a pre-cooled French-pressure-20K chamber, and lysed by compression (Spectronic Instruments/SLM Aminco, 1000 psi, 5min); this procedure was performed twice to lyse cells completely.

V.2.1.3 Purification and concentration of proteins

After centrifugation (10,000 g, 20 min, 4°C), cleared cell lysates were collected and GST-fused proteins purified using Glutathione agrose resin (Sigma-Aldrich). Following dialysis against PBS, proteins were concentrated using Vivaspin columns (Vivascience) and stored at 4 °C.

V.2.2 SDS-PAGE

V.2.2.1 Determination of protein concentration

Protein concentration was determined using a BCA (bicinchoninic acid) Assay Kit (KMF Laborchemie Handels). Briefly, 10 µl of sample was placed on a microplate and incubated for 30 min at 37°C with 200 µl of the solution, which was prepared according to the kit manual. Then, the absorbance was measured at 562 nm wavelength by µQuantTM universal microplate spectrophotometer (Bio-Tek Instruments). The protein concentration was evaluated from the absorbance using a calibration against a protein standard curve.

V.2.2.2 SDS-PAGE (SDS-polyacrylamide gel electrophoresis)

Proteins were separated by discontinuous SDS-PAGE using the Mini-Protean II system (Bio-Rad). The SDS-polyacrylamide gel consists of a stacking gel (4% acrylamide, w/v) and a separating gel (8% acrylamide, w/v)). After polymerization of the gels, the electrophoresis chamber was assembled according to the manufacturer's protocol. Protein samples were diluted with appropriate amount of 5X SDS sample buffer followed by boiling for 5 minutes at 100ºC and 15 µg of total protein of each sample was loaded per well. Gels were run at a constant voltage of 60 V for 20 min and then 90 V until the bromphenol blue line migrated to the bottom of the gel. Gels were either

stained with coomassie blue or subjected to Western blot analysis.

V.2.2.3 Coomassie staining of polyacrylamide gels

Gels were stained with Coomasie Brilliant blue R-250 to detect proteins directly on the polyacrylamide gel for 1 h at room temperature with constant agitation. Then, the gels were incubated in de-staining solution until the background of the gel was nearly transparent.

V.2.3 Western blot analysis

V.2.3.1 Electrophoretic transfer of proteins

Proteins were transferred fromSDS-polymacrylamide gel onto a nitrocellulose membrane (Protran) using a Mini Transblot®-apparatus (Bio-Rad). After equilibration of the polyacrylamide gel in transfer buffer for approximately 5 minutes, a blotting ‘‘sandwich’’ was assembled as described in the manufacturer's protocol. Proteins were transferred at 4°C in transferring buffer at constant voltage (100V for 2 h or 40V overnight).

V.2.3.2 Immunochemical detection of transfered proteins

After electrophoretic transfer, the nitrocellulose membranes were removed from the blotting sandwiches and placed protein side-up in glass vessels. Membranes were washed once in TBST for 5 minutes and subsequently blocked for 1 h in blocking buffer under gentle shaking at room temperature. Incubation with an appropriate antibody diluted in blocking buffer, was performed overnight at 4°C on a shaking platform. The primary antibody solution was removed and membranes were washed 3 x 10 min with TBST under constant shaking. The appropriate horseradish peroxidase (HRP)-conjugated secondary antibody was applied at a concentration varying

from 10 ng/ml to 1 ng/ml in blocking buffer for 90 minutes at room temperature, followed by washing with TBST 5x10 min. Immunoreactivity was visualized using enhanced chemiluminescence detection system (ECL) with extended duration (Pierce Biotechnology). The membrane was covered with detection solution (1:1 mixture of solution I and II) for 2 min, and placed between two plastic foils and exposed to X-ray film (Kodak Biomax-XL, Sigma-Aldrich). Densitometric evaluation of band density

Chemiluminescence was quantified using the image processing software Scion Image (Scion Corporation) or TINA 2.09 software (University of Manchester). The film was scanned and the digitized picture was exported to the image processing program. The quantified data was analyzed using Microsoft Excel software.

V.2.3.3 Stripping and re-probing of immunoblots

For detection of additional proteins on the immunoblots, the nitrocellulose membranes were stripped in stripping buffer for 10 minutes at room temperature. Blots were neutralized for 2 x 5 minutes in 1 M Tris-HCl (pH 7.5) and re-probed.

V.2.4 Subcellular fractionation

V.2.4.1 Preparation of brain homogenates

Mice brains were homogenized on ice in a Dounce homogenizer (Weaton, Telfon pestle) with homogenization buffer containing protease inhibitor cocktail (Roche Diagnostics).

V.2.4.2 Isolation of growth cones from total brain homogenates

Isolation of growth cones fractions was performed according to Pfenninger KH

et al.(Pfenninger et al., 1983). Growth cones were isolated from brains of neonatal (1-3-day-old) mice. Mice brains were gently homogenized with ten stokes in 8x volumes (w:v) of homogenization buffer containing protease inhibitor cocktail (Roche Diagnostics). The homogenates were centrifuged at 1,660 g for 15 min. The low-speed supernatant was carefully tipped off and use further, whereas the low-speed pellets was discarded. Discontinuous sucrose density gradients were prepared in thinwall polyallomer tubes (13x51 mm, V=5 ml; Beckman Instruments). The supernatants were load onto a discontinuous gradient of 0.75/1.0/2.66M and centrifuged at 242,000 g for 40 min using a SW55 Ti Beckman rotor. The fraction at the interface between the load and 0.75 M sucrose was collected and resuspended in homogenization buffer, then pelleted at 100,000 g for 4 min to obtain purifed growth cones. All these procedures were carried out on ice or at 4°C.

V.2.4.3 Isolation of soluble fractions and membrane fractions from total brain homogenates

The brain homogenates were centrifuged at 1,400 g for 10 min to spin down mitochondria and nuclei. Pellets and supernatants were carefully separated. Thereafter, the supernatants were centrifuged at 100,000 g for 30 min. The finally obtained supernatants were enriched in cytosolic proteins and termed soluble fractions. The pellets were resuspended in a minimal volume of TBS buffer and used as total membrane fractions. Protease inhibitor cocktail was added to all fractions and the total protein content was estimated.

V.2.4.4 Isolation of lipid rafts fraction from total membrane fractions

Lipid rafts fractions were defined from membrane fraction as previously described (Leshchyns'ka et al., 2003). Maximum 500 µl of membrane fractions was mixed with 4x volumes of ice-cold 1% Triton X-100 in TBS in polyallomer tubes (14x95 mm, V=14 ml; Bechman Instruments) and incubated for 20 min

on ice. The extracted membrane were mixed with and equal volume of 80% sucrose in 0.2M Na_2CO_3 to a final sucrose concentration of 40%. To create discontinuous gradients the material was overlaid with 2ml 30% in TBS solutione and 1ml 10% sucrose inTBS. Tubes were filled up with TBS buffer and centrifuged at 230,000 g for 17 h. After centrifugation the lipid rafts fractions were collected at the top of the gradient at 10% sucrose, resuspended in TBS buffer and pelleted down by centrifugation at 100,000 g for 1h. The pellets were resuspended in a minimum volume of TBS containing protease inhibitor cocktail. The total protein content was estimated.

V.2.4.5 Detergent fractionation of spectrin from brain homogenates

Fractionation of spectrin into 0.1% Triton X-100-soluble and –insoluble material was performed according to Molitoris *et al.* (Molitoris et al., 1996). Brain homogenates were extracted for 5 min at 4°C with PHEM buffer containing 0.1% Triton X-100 and protease inhibitor cocktail. Samples were then centrifuged for 10 min at 48,000 g at 4°C. Supernatants (un-polymerized spectrin) and pellets (polymerzed spectrin) were analyzed by Western-blot analysis.

V.2.5 Protein-protein binding assay

V.2.5.1 Co-immunoprecipitation

For co-immunoprecipitation experiments, samples containg 1 mg of total protein were lysed with ice-cold RIPA lysis buffer containing protease inhibitor cocktail, for 20 min at 25°C. When indicated, 2mM EGTA, 0.2 mM $CaCl_2$ or 2mM $CaCl_2$ was added to the lysis RIPA buffer. Lysates were centrifuged for 15 min at 20,000 g at 4°C. The supernatants were pre–cleared with 20 µl of protein A agarose beads for 3 hours at 4°C with constant rotating. Afterwards, beads were pelleted down by spinning at 500 x g for 5 minutes and the

supernatant carefully pipetted out into another tube. The supernatants were incubated with polyclonal CHL1 antibodies or non-specific rabbit IgG overnight at 4°C with constant rotating, followed by precipitation with protein A agarose beads for 3 h at 4°C. The beads were pelleted and wash 4 times with ice-cold RIPA buffer. The proteins were eluted from the beads with 5xSDS sample buffer and boilded at 100°C for 10 min. The samples were analyzed by Western-blotting.

V.2.5.2 ELISA protein ligand-binding assay

Purified brain spectrins (0-10 nM) (gift from Prof. Sikorski, AF) were immobilized overnight on 96-well polyvinyl chloride plates (Nunc) in PBS. Wells were then blocked for 1.5 h with PBS containing 3% BSA and incubated with 50 nM GST-tagged recombinant proteins (GST-CHL1-ID or GST-L1-ID) or 50nM GST diluted in PBS with 3% BSA overnight. Plates were washed five times with PBST and incubated for 2 h at room temperature with polyclonal antibodies against GST diluted 1:10,000 in PBST containing 3% BSA. After washing with PBST, wells were incubated with horseradish peroxidase-coupled secondary antibodies in PBST containing 3% BSA for 2 h ,washed five times with PBST, developed with 1 mg/ml o-phenylenediamine dihydrochloride (OPD; PerbioScience). The reaction was stopped with 2.5 M H_2SO_4. The OD was measured at 405 nm.

V.3 Cell biological methods

V.3.1 Cell culature

V.3.1.1 Maintenance of NIH 3T3 cells

NIH 3T3 cells were either grown in 75 cm^2 flasks (Greiner Bio-One) with 20 ml culture medium or in six-well plates (d=35 mm; area=9.69 cm^2, Greiner

Bio-One) with 3 ml medium under constant conditions at 37°C, 5 % CO2 and 90 % relative humidity. Cells were passaged as they reached confluence after 3 days. The medium was removed and the cell layer washed once with HBSS prior to detachment in trypsin/EDTA for 5 min at 37°C. Detached cells were resuspended in fresh medium. For maintenance cells were split 1:3 in fresh medium and seeded in new flasks or six-well plates.

In the presence of 10% DMSO cells were cryoconserved and stored at -80°C.

Therefore, the cell layer was washed with HBSS, trypsinized and collected in NIH 3T3 culture medium. The cell pellet , obtained by centrifugation at 900 g for 5 min at room temperature, was resuspented in NIH 3T3 cell freezing medium containing 20% DCS and 10% DMSO and transferred into cryotubes (Biochrom). The cryotubes were frozen in a freeing container (Nunc) frilled with 100% isopropyl alcohol.To ensure continuous cooling to -80°C with a cooling rate of 1°C per minute. After 24 h the cryotubes were removed from the freezing container and stored at -80 °C. To recultivate cryoconserved cells, thawed cells were immediately transferred into flasks or plates containing prewarmed medium. When the cells were adherent, the culture medium was exchanged.

V.3.1.2 Transient transfection of NIH 3T3 cells

NIH 3T3 cells were transfected using the Lipofectamine 2000 reagent (Invitrogen) according to the manufacturer' protocol. One day prior transfection cells were seeded in six-well plates. When cell density reached 80-90%, the cells were ready for transfection. 2 µg DNA and 10 µl lipofectamine 2000 reagent were used to form DNA-lipid complex for per well in 200µl of serum free DMEM/F12 medium. The DNA-lipid complexes were added to 1 ml cell growth medium without antibiotics.The medium was replaced after overnight incubation, and 24 h after transfection the cells were used for biochemical

analysis.

V.3.1.3 Stable transfection of NIH 3T3 cells

Flp-In-3T3 cells were co-transfected with full-length CHL1 pEF5/FRT/V5-D-TOPO and pOG 44 plasmids using Lipofectamine 2000 reagent according to the manufacturer's instructions. pOG44 is plasmid for expression of a Flp recombinase in mammaliam cells. Flp recombinase can help CHL1 gene to integrate into the genome of Flp-In-3T3 cells at the FRT site to generate stable-expression cell line. The integrated cells are resistant to the hygromycin B. 24h after transfection, the cells were selected in culture medium containing 200 µg/ml hygromycin B (Invitrogen) for 3 to 4 weeks. Single clones were selected and verified by Western-blot analysis.

V.3.1.4 Primary cultures of hippocampal neurons

The experiments with primary cultures of hippocampal neurons were performed in cooperation with Dr. Leshchyns'ka and Dr. Sytnyk.

Coating of coverslips

Primary hippocampal neurons were grown on glass coverslips (15 mm, Carl Roth) coated with poly-D-lysine (PDL). The coating procedure required several incubation and washing steps which were performed with gentle shaking in a glass Erlenmeyer flask in solutions with a volume of 100 ml each. Coverslips were then incubated for 30 min with 3 M HCl at room temperature. Afterwards, they were washed twice for 10 min with sterile distilled water and incubated overnight with acetone at 4°C. This was followed by five washing steps for 10 min washer with sterile ddH2O and then twice with absolute ethanol. To sterilize coverslips, they were heated for 2 h at 200°C. After cooling down to room temperature, coverslips were incubated overnight in sterile 0.01 % PDL

in PBS at 4°C and afterwards washed three times with ddH2O Thereafter, coverslips were dried uncovered in a laminar flow hood under UV light for 30 min. The coated coverslips were stored in a sterile tube at room temperature until use.

Preparation and cultivation of hippocampal neurons

Cultures of hippocampal neurons were prepared from 1-3-day-old mice. Mice were decapitated and brains were removed from the skull. Briefly hippocampi were extracted, placed in cold dissection solution and cut into 1 mm thick pieces. Hippocampi were washed once with neurobasal^{TM}-A medium and treated with a digestion solution containing papain and DNase I for 30 min at 30°C. The digestion solution was removed and hippocampi suspended in dissection solution. Hippocampi were carefully dispersed into a homogeneous suspension by trituration in dissociation solution with glass Pasteur pipettes having successively smaller diameters. The suspension was centrifuged at 80 g for 25 min at room temperature. The pelleted cells were resuspended in dissociation solution. Cell numbers were estimated using a Neubauer counting cell chamber (Carl Roth). The cells were then seeded on coverslips coated with 0.01 % PDL (see 2.4.1) and maintained in growth medium at 37°C in a constant CO_2 atmosphere of 5 % and 90 % relative humidity.

V.3.2 Immunocytochemistry

V.3.2.1 Immunofluorescence labeling

Indirect immunofluorescence labeling was performed as described previously (Leshchyns'ka et al., 2003). All steps were performed at room temperature. Neurons were fixed in 4 % PFA in PBS for 15 min to cross-link and preserve proteins in their native conformation. This fixation procedure does not permeabilize membranes. Subsequently, cells were washed and blocked in 1

% BSA in PBS for 20 min. Antibodies against the CHL1 extracellular domain were applied in 1 % BSA in PBS for 30 min and detected with fluorochrome-coupled secondary antibodies applied for 30 min. The neurons were postfixed for 5 min in 2 % PFA diluted in PBS. To detect intracellular proteins, cells permeabilized with 0.25 % Triton X-100 in PBS for 5 min, then blocked with 1 % BSA in PBS for 20 min. Antibodies were applied in 1 % BSA in PBS for 2 h and then detected with secondary antibodies applied for 45 min.

V.3.2.2 Image acquisition and manipulation

Coverslips were embedded in Aqua-Poly/Mount (Polysciences) and fixed on microscope slides over night at room temperature. Immunofluorescence images were acquired at room temperature using a confocal, laser-scanning microscope LSM510, LSM510 software (version 3) and oil Plan-Neofluar 40x objective (numerical aperture 1.3) at 3x digital zoom (Zeiss). Contrast and brightness of the images were further adjusted in Corel Photo-Paint 9 (Corel Corporation).

V.3.3 Quantification of neurite length (neurite outgrowth assay)

Neurons seeded on coverslips coated with PDL were incubated for 1 h before further components were added. When indicated lipid biosynthesis inhibitors were applied to the culture medium 1 h before stimulation with either CHL1 polyclonal antibodies or non-specific rabbit IgG for 24 h. After incubation, cells grown on the coverslips were treated with 4 % PFA in PBS for 30 min at room temperature and washed twice with PBS. Coverslips were fixed on the microscope slide over night at room temperature. The cells were imaged using an Axiophot 2 microscope equipped with a Plan-Neofluar 40x objective (numerical aperture 0.75), AxioCam HRc digital camera and AxioVision software version 3.1 (Zeiss). Neurite length was measured with the image

processing software ImageJ version 1.34s (open source, National Institutes of Health, USA). For each experimental value at least 250 neurons with neurites longer than the cell body diameter were measured. Results were statistically evaluated using two-tailed *t*-test. Results are presented as the mean ± SEM.

V.3.4 Cell surface biotinylation

Wild type or mutant CHL1 constructs were transfected into NIH 3T3 cells using lipofectamine 2000 (Invitrogen) grown in 6-well plates. After 24 h after transfection, CHL1 polyclonal antibodies against the extracellular domain (1: 200, v:v) were applied to cells for 10 min at 37 °C. The cells were washed twice with ice-cold PBS containing 1 mM $CaCl_2$ and 0.5 mM $MgCl_2$, and then biotinylated using 0.5 mg/ml of EZ-Link Sulfo-NHS-LC-Biotin (Pierce Biotechology) incubated for 30 min at 4°C. The reactions were stopped by adding 50 mM glycine and incubate for 10 min at 4°C. After washing twice with ice cold PBS, the cells were scraped into 166 µl per well warm precipitation buffer with complete protease inhibitor and phosphostop (Roche Diagnostics). The resulting solution was then diluted with 833µl per well of cold PBS with 1% Triton X-100 and centrifuged at 20,000 g for 20 min at 4°C. To precipitate biotinylated proteins, supernatants containing equal amounts of protein were mixed with 100 µl neutravidin agarose beads (Pierce Biotechnology) overnight at 4°C with rotation. After washing 3 times with PBST, the precipitates were boiled in 5xSDS sample buffer, subjected to SDS-PAGE and Western-blot analysis. 10 µM nifedipine and 5µM pimozide (Alomone Laboratories) were applied for 10 min at 37 °C before stimulation.

VI RESULTS

VI.1 CHL1 associates with βII spectrin independently of ankyrin-B

The intracellular domain of CHL1 contains a motif FIGQ(A)Y, which is highly conserved across the L1 family of adhesion molecules. This motif is recognized by ankyrin in several L1 family members, including L1 and neurofascin (Garver et al., 1997; Jenkins et al., 2001). To analyze whether CHL1 also associates with ankyrin, co-immunoprecipitation experiments were performed. Ankyrin-B co-immunoprecipitated with CHL1 from lysates of brains of 1-3-day-old mice (Fig. VI.1A). Thus, CHL1 associated with ankyrin-B in developing brains. This observation agreed with published data showing that CHL1 regulates membrane targeting of another ankyrin isoform, ankyrin-G, in HEK293 cells (Buhusi et al., 2003).

Further analysis showed that spectrin, a prominent binding partner of ankyrin, also associated with CHL1 (Fig. VI.1A). Interestingly, while βII spectrin readily co-immunoprecipitated with CHL1, very low levels, if any, of βI spectrin associated with CHL1 in brain lysates (Fig. VI.1A). These observations suggest selectivity in CHL1 binding to spectrin isoforms.

Double immunofluorescence labeling of cultured 1-day-old hippocampal neurons with antibodies against CHL1 and βII spectrin showed that CHL1 and βII spectrin were expressed along neurites, growth cones and in soma of neurons (Fig. VI.1B). Distributions of CHL1 and βII spectrin in developing neurons partially overlaped further indicating that CHL1 and βII spectrin can engage in physical interactions.

Phosphorylation of the tyrosine residue within the ankyrin binding motif

FIGQ(A)Y have been reported to abolish the ankyrin-binding activity in L1 and neurofascin (Garver et al., 1997; Jenkins et al., 2001). To analyze whether the association of CHL1 with ankyrin-B and βII spectrin is modulated by phosphorylation, co-immunoprecipitation experiments were carried out either in the absence or presence of vanadate, an inhibitor of tyrosine phosphatases. The efficiency of the co-immunoprecipitation of ankyrin-B with CHL1 was inhibited in the presence of vanadate by approximately 50% (Fig. VI.1C) suggesting that tyrosine phosphorylation reduces the interaction between CHL1 and ankyrin-B. In contrast, vanadate does not affect the co-immunoprecipitation of βII spectrin with CHL1 (Fig. VI.1C).

A possible explanation for this observation is that CHL1 associates with βII spectrin in an ankyrin-independent manner. To investigate whether CHL1 and βII spectrin can interact directly, αIIβII spectrin purified from bovine brains was immobilized on plastic, and its ability to capture recombinant GST-tagged intracellular domain (ID) of CHL1 was measured by ELISA. CHL1-ID bound to spectrin αIIβII in a concentration-dependent manner (Fig. 1D). GST tag alone did not bind to αIIβII spectrin (Fig. VI.1D). Interestingly, αIIβII spectrin was also able to bind L1-ID, which has approx. 40% similarity with CHL1-ID (Fig. VI.1D). The affinity of L1-ID binding to αIIβII spectrin was, however, much lower than that of CHL1-ID.

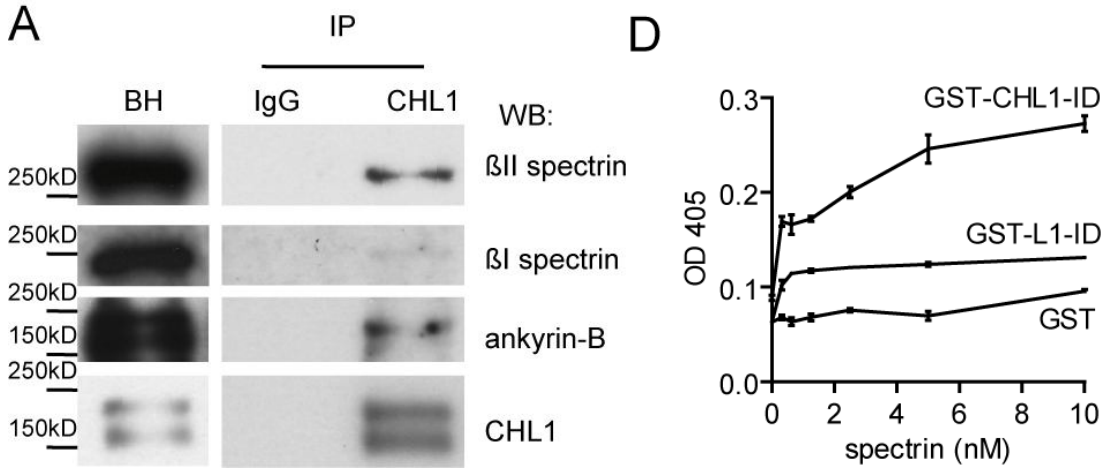

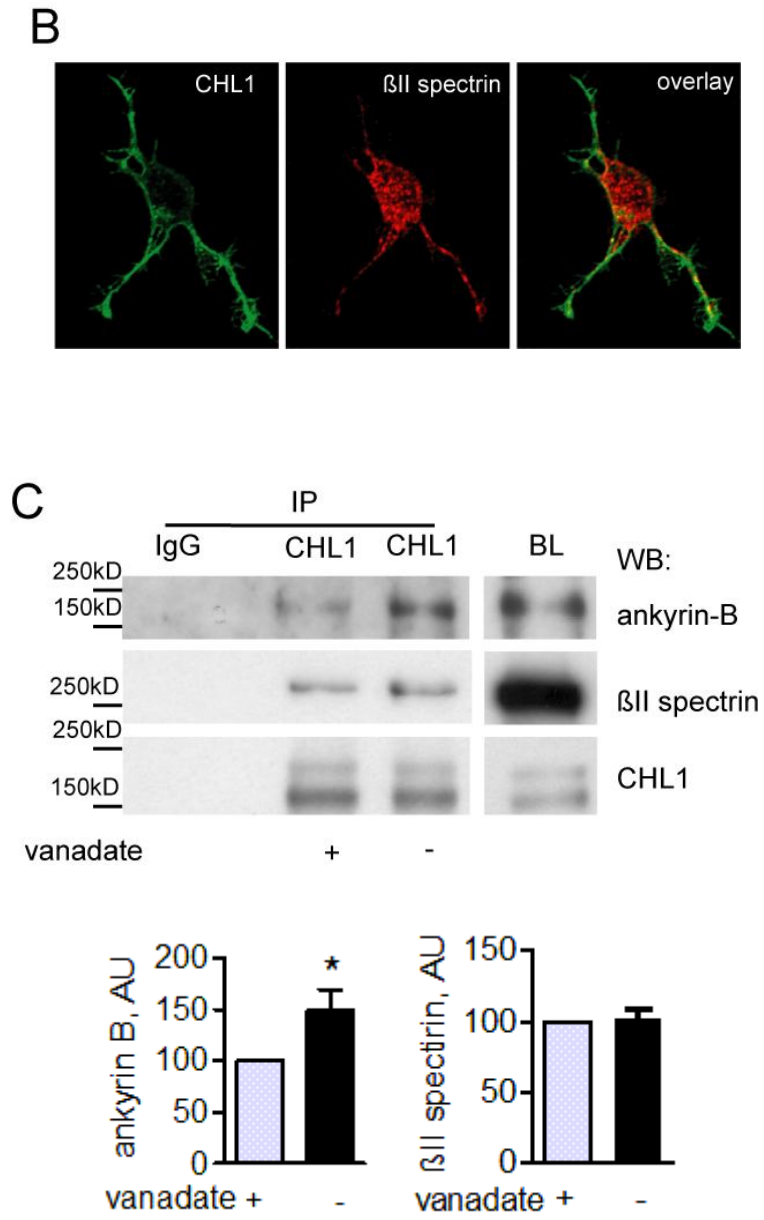

Figure VI.1. CHL1 interacts with βII spectrin independently of ankyrin-B.

(A) CHL1 was immunoprecipitated (IP) from brain lysates from 1-3-day-old mice. Mock immunoprecipitation with nonspecific rabbit immunoglobulins (IgG) was performed for control. Brain homogenates (BH) and immunoprecipitates were analyzed by Western blot as indicated. Spectrin βII and ankyrin-B, but not βI spectrin coimmunoprecipitated with CHL1. (B) 1-day-old cultured hippocampal neurons co-labeled by indirect immunofluorescence for CHL1 and βII spectrin are shown. Note that CHL1 and βII spectrin partially colocalize along neurites and in growth cones of neurons. (C) CHL1 was immunoprecipitated (IP) from brain lysates from 1-3-day-old mice in the presence or absence of vanadate. Mock immunoprecipitation with nonspecific rabbit immunoglobulins (IgG) was performed for control. Brain homogenates (BH) and immunoprecipitates were analyzed by Western blot as indicated. Note, that vanadate inhibited co-immunoprecipitation of ankyrin-B with CHL1. Co-immunoprecipitation of βII spectrin with CHL1 was not influenced by vanadate. Graphs show quantitation of blots (mean values ± SEM, n=3 experiments) with optical density in the presence of vanadate set to 100%. *, P< 0.05, paired *t*

test. (D) αIIβII spectrin was immobilized on plastic surfaces at increasing concentrations and assayed by ELISA for its ability to bind GST-CHL1-ID or GST-L1-ID (50 nM). GST (50 nM) served as a control. Intracellular domain (ID). Mean values (OD405) ± SEM (n=3) are shown.

VI.2 Targeting of βII spectrin and ankyrin-B to the growth cones is impaired in CHL1-/- mice.

CHL1 has been shown to be involved in the regulation of growth cone morphology and neuritogenesis (Schlatter et al., 2008). Remodeling of the cytoskeleton in growth cones of growing neurites is critical for these processes. To investigate whether CHL1 is involved in regulation of the levels of spectrin and ankyrin in growth cones, we compared levels of these proteins in growth cones isolated from the brains of CHL1+/+ and CHL1-/- mice. Levels of βII spectrin and ankyrin-B, but not βI spectrin were reduced in growth cones isolated from the brains of CHL1-/- mice when compared to CHL1+/+ growth cones (Fig. VI.2B). This observation suggests that CHL1 is involved in targeting βII spectrin and ankyrin-B to the growth cones. Interestingly, levels of βII spectrin and ankyrin-B were increased in brain homogenates of CHL1-/- versus CHL1+/+ mice (Fig. VI.2A), probably reflecting a compensatory reaction to the abnormal function of these proteins. In contrast, levels of βI spectrin were not changed in brain homogenates from CHL1-/- mice (Fig. VI.2A).

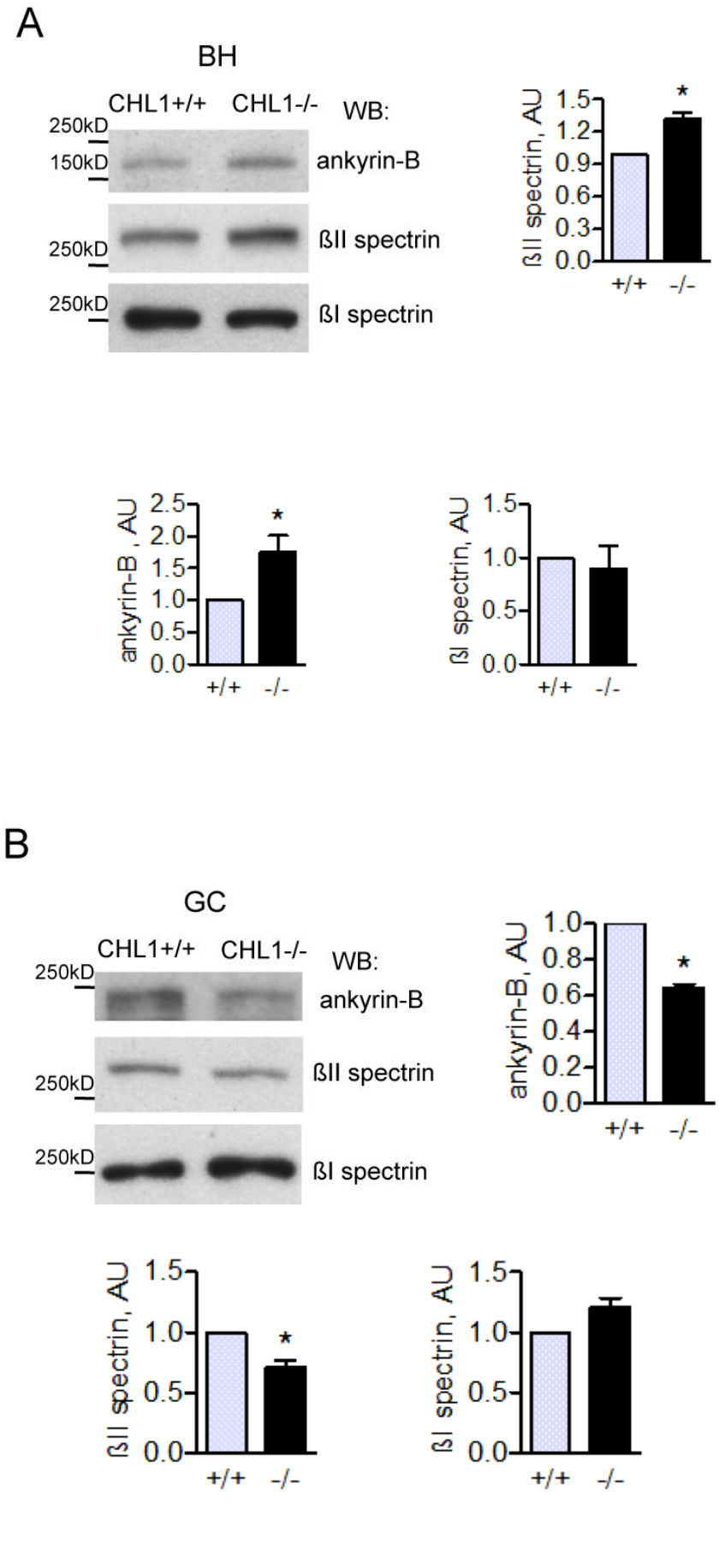
A
BH
CHL1+/+
CHL1-/-
WB:
250kD
150kD
ankyrin-B
250kD
ßII spectrin
250kD
ßI spectrin
ßII spectrin, AU
1.5
1.2
0.9
0.6
0.3
0.0
+/+
-/-
*
ankyrin-B, AU
2.5
2.0
1.5
1.0
0.5
0.0
ßI spectrin, AU
B
GC
ankyrin-B, AU
ßII spectrin, AU
ßI spectrin, AU

Figure VI.2. Targeting of βII spectrin and ankyrin-B to growth cones is impaired in CHL1-/- mice. (A,B) Brain homogenates (BH) and growth cones (GC) from 1-3-day-old CHL1+/+ and CHL1-/- mice were analyzed by Western blot (WB) as indicated. Note that the levels of ankyrin-B and βII spectrin are increased in CHL1-/- vs. CHL1+/+ brain homogenates (A) and reduced in CHL1-/- vs. CHL1+/+ growth cones (B). The levels of βI spectrin are similar in brain homogenates of mice of both genotypes (A) and slightly increased in CHL1-/- vs. CHL1+/+ growth cones (B). Graphs show quantitation of blots (mean values ± SEM, n=3). AU, arbitrary units. *, $P < 0.05$, paired *t* test.

VI.3 Cysteine 1102-dependent targeting of CHL1 to lipid rafts promotes the association of βII spectrin with lipid rafts

Lipid microdomains, called lipid rafts, play an important role in the remodeling of the cytoskeleton beneath the cell surface plasma membrane (Kamiguchi, 2006). To analyze whether CHL1 plays a role in regulating βII spectrin levels in lipid rafts, CHL1+/+ and CHL1-/- total membranes were extracted with 1% Triton-X100 and used to isolate lipid rafts by floatation in a sucrose density gradient. Western blot analysis showed that CHL1 was present in lipid rafts (Fig. VI.3A). Interestingly, we found that βII spectrin was enriched in the lipid raft fraction when compared to total brain homogenates, the total membrane fraction and the fraction containing soluble proteins (Fig. VI.3A). Levels of βII spectrin were reduced in CHL1-/- lipid rafts by approximately 35% when compared to CHL1+/+ lipid rafts (Fig. VI.3A). Levels of lipid raft-associated ankyrin-B were, however, increased in CHL1-/- brains by approximately 50% when compared to CHL1+/+ brains (Fig. VI.3A). These observations thus suggested that CHL1 was involved in targeting of βII spectrin to lipid rafts independently of ankyrin-B. While βIII spectrin was also enriched in lipid rafts, its levels were not affected by CHL1 deficiency. Similarly, levels of the lipid raft marker proteins $p59^{fyn}$ and contactin were similar in lipid rafts isolated from CHL1 +/+ and CHL1 -/- brains, indicating that CHL1 deficiency does not affect the overall raft composition and that lipid rafts are isolated with the same efficacy (Fig. VI.3A).

Targeting of adhesion molecules to lipid rafts has been shown to be dependent on the palmitoylation of their intracellular domains (Niethammer et al., 2002). The intracellular domain of mouse CHL1 contains a cysteine residue at position 1102 (Cys1101 in human CHL1). To investigate whether this cysteine plays a role in the association of CHL1 with lipid rafts, cysteine 1102 was exchanged to serine by site directed mutagenesis. Wild type (WT) non-mutated CHL1 and the CHL1C1102S mutant were stably transfected into NIH 3T3 cells which were then used for lipid raft isolation. Western-blot analysis of the lipid rafts from the transfected cells showed that only CHL1WT but not CHL1C1102S was detectable in lipid rafts (Fig. VI.3B). Expression levels of CHL1C1102S analyzed in total cell lysates were, however, similar to that of CHL1WT. Therefore, reduced levels of CHL1C1102S in lipid rafts were not due to a decrease in the overall expression levels of this mutant. Our data thus suggest that palmitoylation of cysteine 1102 is critical for targeting of CHL1 to lipid rafts (Fig. VI.3B).

Interestingly, levels of βII spectrin were lower in lipid rafts isolated from CHL1C1102S transfected cells when compared to cells transfected with CHL1WT (Fig. VI.3B). This observation is in agreement with our hypothesis that the recruitment of βII spectrin to lipid rafts is regulated by CHL1. Levels of the lipid raft marker protein $p59^{fyn}$ were similar in lipid rafts isolated from both cell lines (Fig. VI.3B) indicating similar efficiencies of lipid raft isolation.

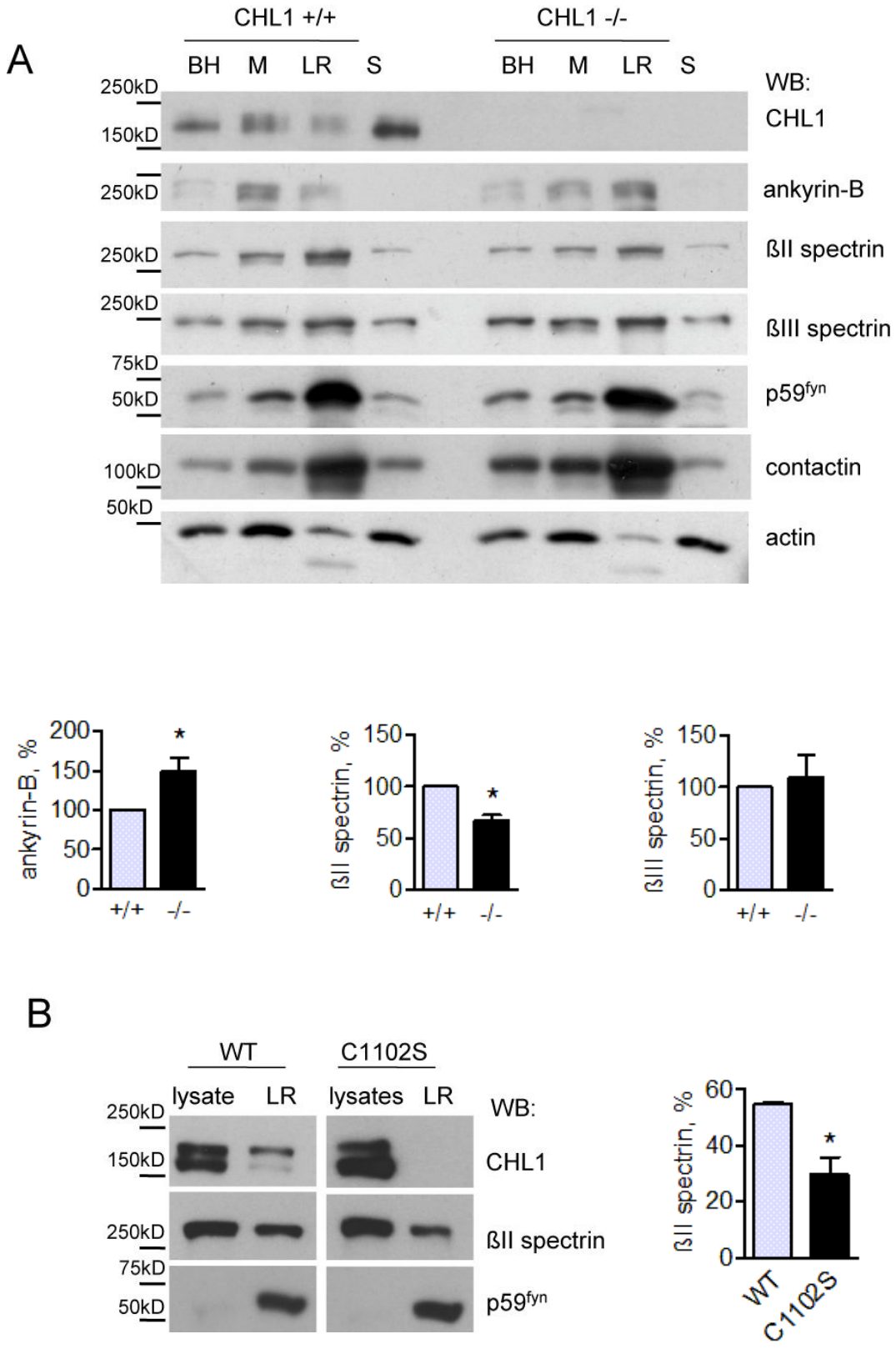

Figure VI.3. CHL1 regulates levels of βII spectrin in lipid rafts.

(A) Brain homogenates (BH), membrane fractions (M), lipid raft fractions (LR) and soluble fractions (S) from CHL1+/+ and CHL1-/- brains were probed by Western blot (WB) as indicated. Note, that CHL1 is

preset in lipid rafts. Soluble fraction contains CHL1 released from the surface by proteolytic cleavage of the extracellular domain. Note that the levels of βII spectrin are reduced, while levels of ankyrin-B are increased in lipid rafts from CHL1-/- vs. CHL1 +/+ mice. The levels of βIII spectrin are similar in lipid rafts of both genotypes. Labeling for lipid raft markers p59fyn and contactin was performed to check the efficiency of lipid raft isolation. Actin served as a loading control. Graphs show quantitation of blots (mean values ± SEM, n=3) with optical density for CHL1+/+ set to 100%. *, P < 0.05, paired t test. (B) Lipid rafts were isolated from NIH 3T3 cells stably transfected with CHL1WT or CHL1C1102S. Cell lysates and lipid rafts (LR) were probed by Western blot (WB) as indicated. Labeling for a lipid raft marker p59fyn was performed to check the efficiency of lipid raft isolation. Note that CHL1C1102S is not detectable in lipid rafts. Levels of βII spectrin are reduced in lipid rafts isolated from CHL1C1102S vs. CHL1WT transfected cells. Graph shows levels βII spectrin in lipid rafts normalized to βII spectrin levels in cell lysates (mean values ± SEM, n=3). *, P < 0.05, paired *t* test.

VI.4 Levels of polymerized βII spectrin are increased in CHL1-/- mice

Our observations on the role of CHL1 in targeting βII spectrin to lipid rafts suggest that CHL1 may play a role in βII spectrin meshwork remodeling. To investigate this hypothesis, we examined the impact of CHL1 deficiency on the detergent insolubility of spectrin – a measure of its incorporation into a detergent-resistant submembrane cytoskeleton (Leshchyns'ka et al., 2003). CHL1+/+ and CHL1-/- brain homogenates were extracted with 0.1% Triton X-100 to obtain 0.1% Triton X-100 insoluble and soluble fractions, which were then analyzed by Western blot. This analysis showed that levels of 0.1% Triton X-100 insoluble βII spectrin were increase, while levels of 0.1% Triton X-100 soluble βII spectrin were decreased in CHL1-/- brains, indicating that polymerization of βII spectrin is increased in CHL1-/- brains (Fig. VI.4). The levels of ankyrin-B were increased both in 0.1% Triton X-100 soluble and insoluble fractions from CHL1-/- brains in agreement with our data on the overall increased expression of this protein in CHL1-/- brains (Fig. VI.2A). The ratio of insoluble to soluble ankyrin-B levels was similar for both genotypes (Fig.

VI.4), suggesting that CHL1 regulates βII spectrin polymerization levels in an ankyrin-B independent manner. The ratio of insoluble to soluble actin was also not affected by CHL1 deficiency, indicating that the overall cytoskeleton composition is not affected by CHL1 deficiency.

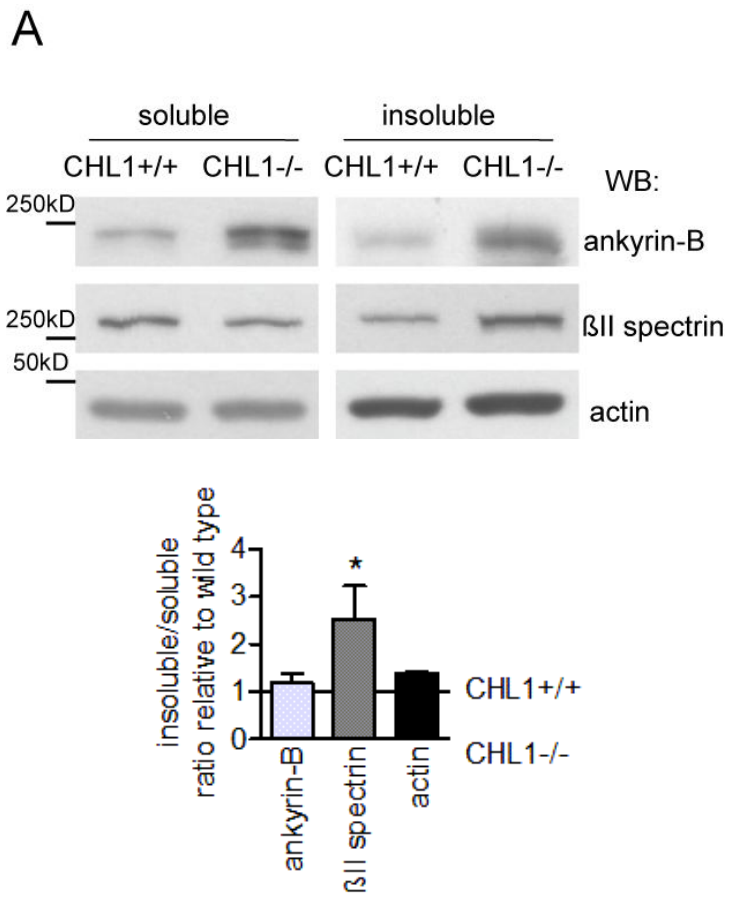

Figure VI.4. Polymerization of the βII spectrin meshwork is increased in CHL1-/- brains.
(A-B) CHL1+/+ and CHL1-/- brain homogenates were extracted with 0.1% Triton X-100 and analyzed by Western blot (WB) as indicated (A). Note that levels of detergent soluble βII spectrin are reduced, while levels of detergent insoluble βII spectrin are increased in CHL1-/- brains. Graph (B) shows the ratio of detergent insoluble to soluble protein levels in CHL1-/- brains normalized to CHL1+/+ values set to 1 (mean values ± SEM, n=3). Note that the ratio of 0.1% Triton X-100 insoluble to soluble βII spectrin is increased in CHL1-/- vs. CHL1+/+ brains. *, $P < 0.05$, paired *t* test.

VI.5 Clustering of CHL1 induces CHL1 internalization and detachment of spectrin from membranes in a lipid raft dependent manner

Clustering of CHL1 at the neuronal cell surface is a neurite outgrowth-promoting signal (Hillenbrand et al., 1999b). Since our data indicate that CHL1 is involved in the regulation of the βII spectrin-containing cytoskeleton, we analyzed whether clustering of CHL1 changes the association of βII spectrin with the surface membranes. NIH 3T3 cells were transfected with CHL1WT or CHL1C1102S to assess the role of lipid rafts in the CHL1-mediated cytoskeleton reorganization. The cells were then treated with control non-specific immunoglobulins or CHL1 antibodies to induce clustering of CHL1 at the cell surface. To analyze levels of βII spectrin attached to the cytoplasmic leaflet of the cell surface membrane by interaction with transmembrane proteins, cell surface exposed proteins in transfected 3T3 cells were biotinylated and separated from the total protein pool. The levels of βII spectrin that was co-purified with the cell surface proteins were then analyzed by Western blot. This analysis showed that after application of CHL1 antibodies to CHL1WT transfected cells, the amount of surface membrane-associated βII spectrin decreased by approximately 50% (Fig. VI.5A). This effect was blocked in CHL1C1102S transfected cells, indicating that lipid raft localization of CHL1 is necessary for CHL1-dependent detachment of βII spectrin from the cell surface plasma membrane (Fig. VI.5A). Antibody treatment did not alter the overall protein expression of βII spectrin (Fig. VI.5B). In contrast to βII spectrin, levels of membrane-associated clathrin (Fig. VI.5A) or Na,K ATPase (not shown) did not significantly change after CHL1 antibody application.

Interestingly, we found that application of CHL1 antibodies also resulted in an approximately 40% decrease in the levels of CHL1WT at the cell surface (Fig.

VI.5A). The total levels of full length CHL1WT were not changed in CHL1 antibody treated cells (Fig. VI.5B), excluding possible shedding of CHL1WT from the cell surface. Thus, we conclude that clustering of CHL1 results in its internalization. Internalization of the CHL1C1102S mutant was blocked (Fig. VI.5A), suggesting that the association of CHL1 with lipid rafts is required for its internalization.

To investigate whether the detachment of βII spectrin from the cell surface plasma membrane is due to the dissociation of CHL1/βII spectrin complex, co-immunoprecipitation experiments were performed. CHL1WT and CHL1C1102S were immunoprecipitated from the transfected 3T3 cells either treated or non-treated with CHL1 antibodies. Indeed, levels of βII spectrin that co-immunoprecipited with CHL1WT from CHL1 antibody-treated cells was reduced by approximately 50% when compared to control cells (Fig. VI.5C), indicating that clustering of CHL1 is accompanied by the disassociation of the CHL1/βII spectrin complex within 10 min after antibody application. In contrast, the association of CHL1C1102S with βII spectrin was not affected following CHL1 antibody application (Fig. VI.5C). This observation indicates that the association of CHL1 with lipid rafts is required for CHL1/βII spectrin complex disassembly in response to CHL1 clustering at the cell surface.

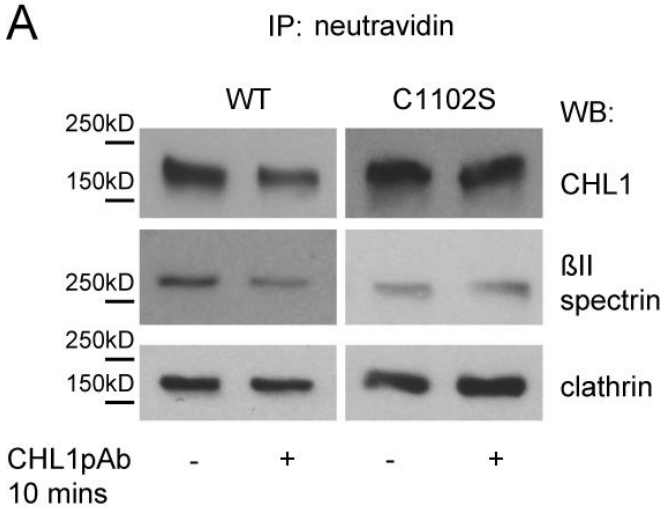

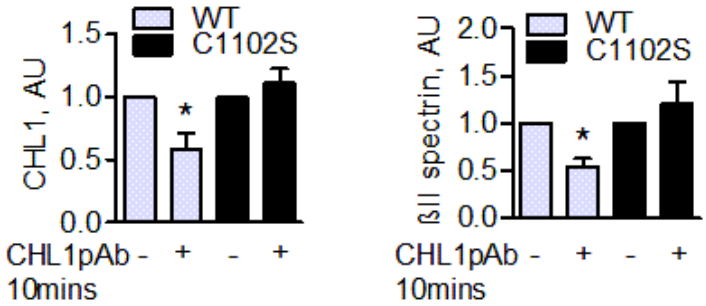
WT
C1102S
CHL1, AU
1.5
1.0
0.5
0.0
*
CHL1pAb - + - +
10mins
WT
C1102S
ßII spectrin, AU
2.0
1.5
1.0
0.5
0.0
*
CHL1pAb - + - +
10mins

B

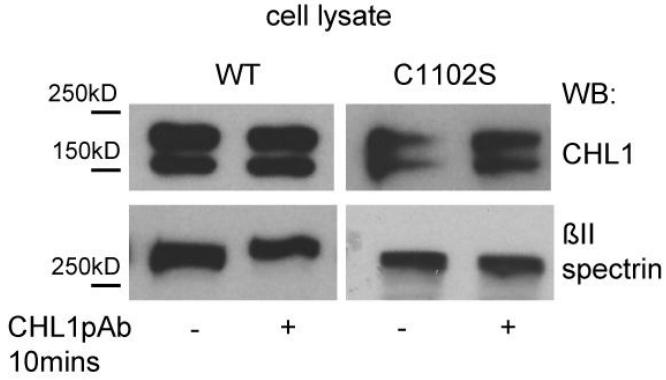
cell lysate
WT
C1102S
250kD
150kD
250kD
WB:
CHL1
ßII
spectrin
CHL1pAb - + - +
10mins

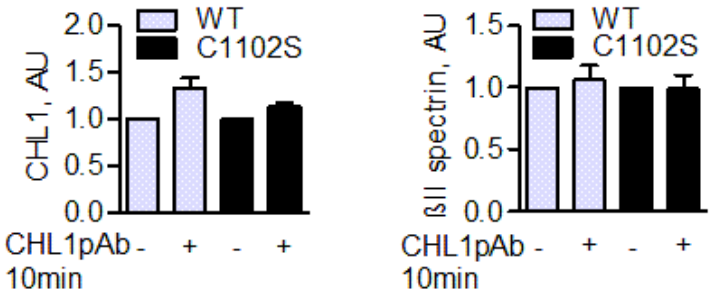
WT
C1102S
CHL1, AU
2.0
1.5
1.0
0.5
0.0
CHL1pAb - + - +
10min
WT
C1102S
ßII spectrin, AU
1.5
1.0
0.5
0.0
CHL1pAb - + - +
10min

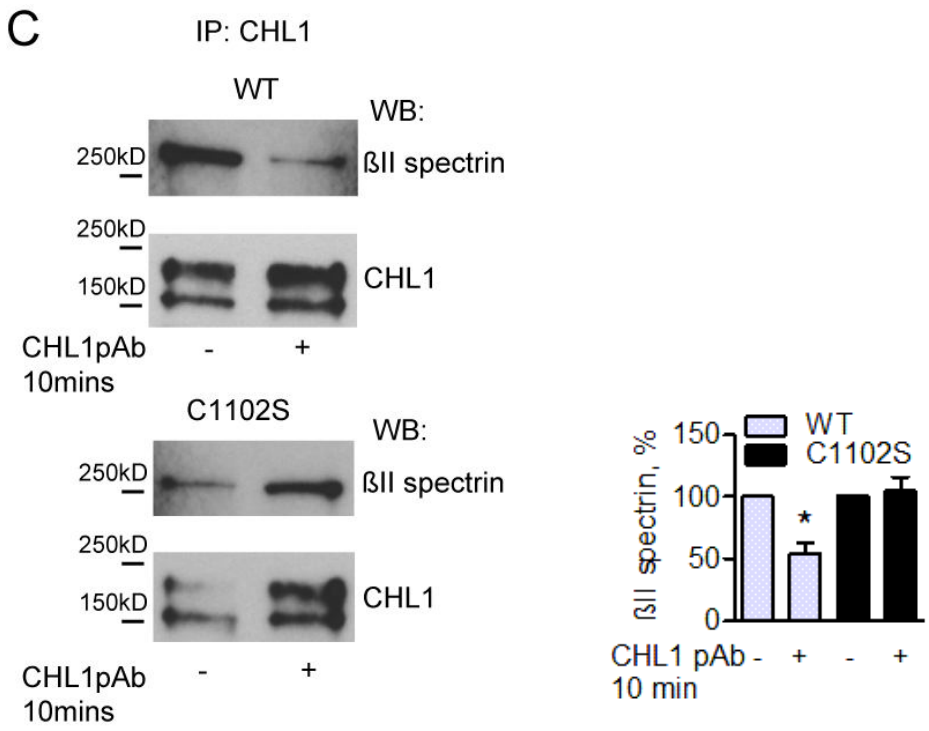

Figure VI.5. Clustering of CHL1 induces its internalization, disassembly of the CHL1/βII spectrin complex and detachment of βII spectrin from membranes.

(A-B) NIH 3T3 cells transfected with CHL1WT or CHL1C1102S were treated with CHL1 polyclonal antibodies for 10 min. Cell surface proteins were then biotinylated and immunoprecipitated with neutravidin-coupled agarose beads after the cell lysis. Cell lysates (B) and immunoprecipitates (A) were analyzed by Western blot (WB) as indicated. Note that the cell surface levels of CHL1WT but not CHL1C1102S are reduced after clustering of CHL1. The levels of the cell surface protein-associated βII spectrin are also reduced after clustering of CHL1 in CHL1WT but not in CHL1C1102S transfected cells. Clustering of CHL1 does not affect the levels of clathrin associated with cell surface proteins. The total levels of CHL1 and βII spectrin are similar in cell lysates of CHL1WT or CHL1C1102S transfected cells either treated or non-treated with CHL1 antibodies. Graphs show quantitation of blots with signals in control cells set to 1 (mean values ± SEM, n=3). *, $P < 0.05$, paired *t* test. (C) CHL1 was immunoprecipitated from NIH 3T3 cells transfected with CHL1WT or CHL1C1102S and either treated or non-treated with CHL1 polyclonal antibodies for 10 min. Note that the co-immunoprecipitation of βII spectrin with CHL1WT is reduced in CHL1-antibody treated cells. The co-immunoprecipitation of βII spectrin with CHL1C1102S was not affected after CHL1 clustering with antibodies. Graph shows quantitation of the blots (mean values ± SEM, n=3) with signals in control CHL1WT transfected cells set to 100%. The levels of the co-immunoprecipitated βII spectrin were normalized to the levels of the immunoprecipitated CHL1. *, $P < 0.05$, paired *t* test.

VI.6 CHL1-βII complex formation and CHL1 internalization are regulated by Ca^{2+}

Since clustering of the immunoglobulin superfamily adhesion molecules, such as NCAM and L1, is known to be associated with the Ca2+ influx (Bodrikov et al., 2008; Williams et al., 1992b), we analyzed whether changes in Ca2+ concentration could be a signal for the CHL1/βII spectrin complex disassembly. CHL1 was immunoprecipitated from brain lysates either in the presence of Ca^{2+} sequestering agent EGTA, or in the presence of various concentrations of Ca^{2+}. The highest co-immunoprecipitation efficiency of βII spectrin with CHL1 was observed in the presence of EGTA, whereas co-immunoprecipitation efficiency was reduced by approximately 50% and 80% when 0.2mM Ca^{2+} and 2mM Ca^{2+} were added to the brain lysates, respectively (Fig. VI.6A, B). These results thus suggest that an increase in Ca^{2+} concentration leads to dissociation of the CHL1/βII spectrin complex, which may facilitate CHL1 internalization.

The analysis of CHL1 immunoprecipitates for the presence of elements of the endocytic machinery showed that the components of the clathrin-dependent pathway, clathrin and AP2, were bound to CHL1 in the presence of EGTA (Fig. VI.6A), in agreement with our previous report (Leshchyns'ka et al., 2006). Interestingly, however, the association of clathrin and AP2 with CHL1 was also reduced in the presence of Ca^{2+} (Fig. VI.6A,B), suggesting that clathrin and AP2 are not involved in CHL1 endocytosis following CHL1/βII spectrin complex disassembly. In search for other components of the endocytic machinery, we found that flotilin-1, a component of lipid raft-dependent and clathrin-independent endocytotic machinery (Glebov et al., 2006), was also associated with CHL1 in brain lysates in the presence of EGTA (Fig. VI.6A,B). This association was further potentiated in the presence of Ca^{2+} (Fig. VI.6A,B).

The combined observations thus suggest that CHL1 is endocytosed via flotillin-dependent lipid raft mediated pathway.

T- and L-type VDCC are present at high level in lipid rafts (Bodrikov et al., 2008). That is why, next, we analyzed whether Ca^{2+} influx via these channels plays a role in CHL1 endocytosis. Cell surface biotinylation was used to compare the levels of CHL1WT at the cell surface in cells pre-incubated with nifedipine, an L-type VDCC inhibitor, and pimozide, a T-type VDCC inhibitor. Application of CHL1 antibodies resulted in the internalization of CHL1WT in control and pimozide-treated cells, but not in cells incubated with nifedipine (Fig. VI.6C). The overall expression of CHL1 was not altered by VDCC inhibitors as shown by Western blot analysis of the cell lysates (Fig. VI.6D). In contrast to CHL1, levels of cell surface, membrane-associated clathrin or Na,K ATPase were not changed after CHL1 antibody application both in control and VDCC inhibitor- treated cells (Fig. VI.6C). Thus, the endocytosis of CHL1 depends on the Ca^{2+} influx via L-type calcium channels.

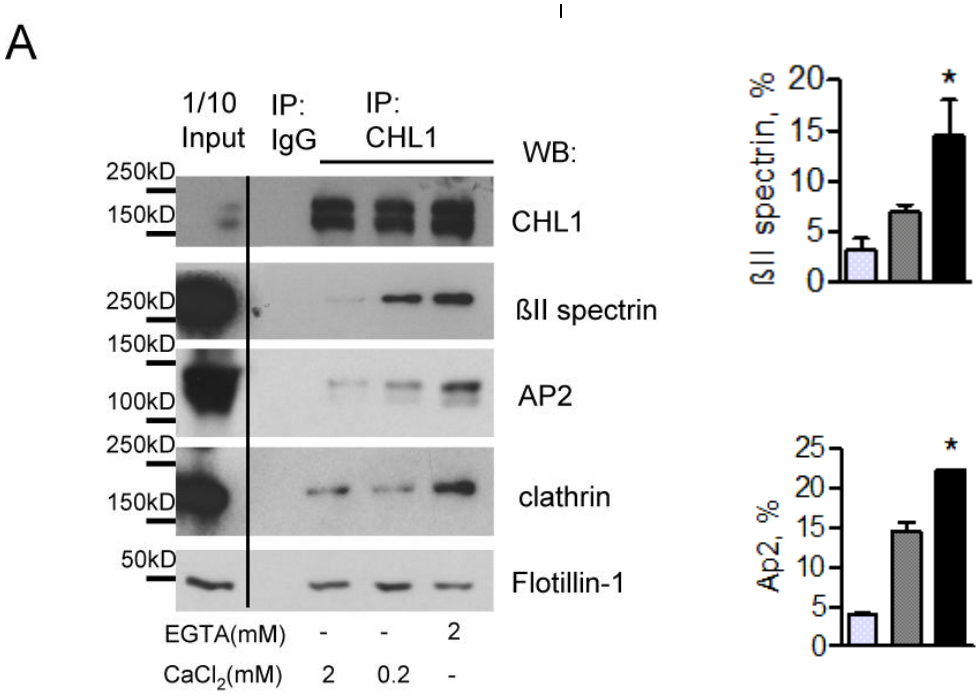

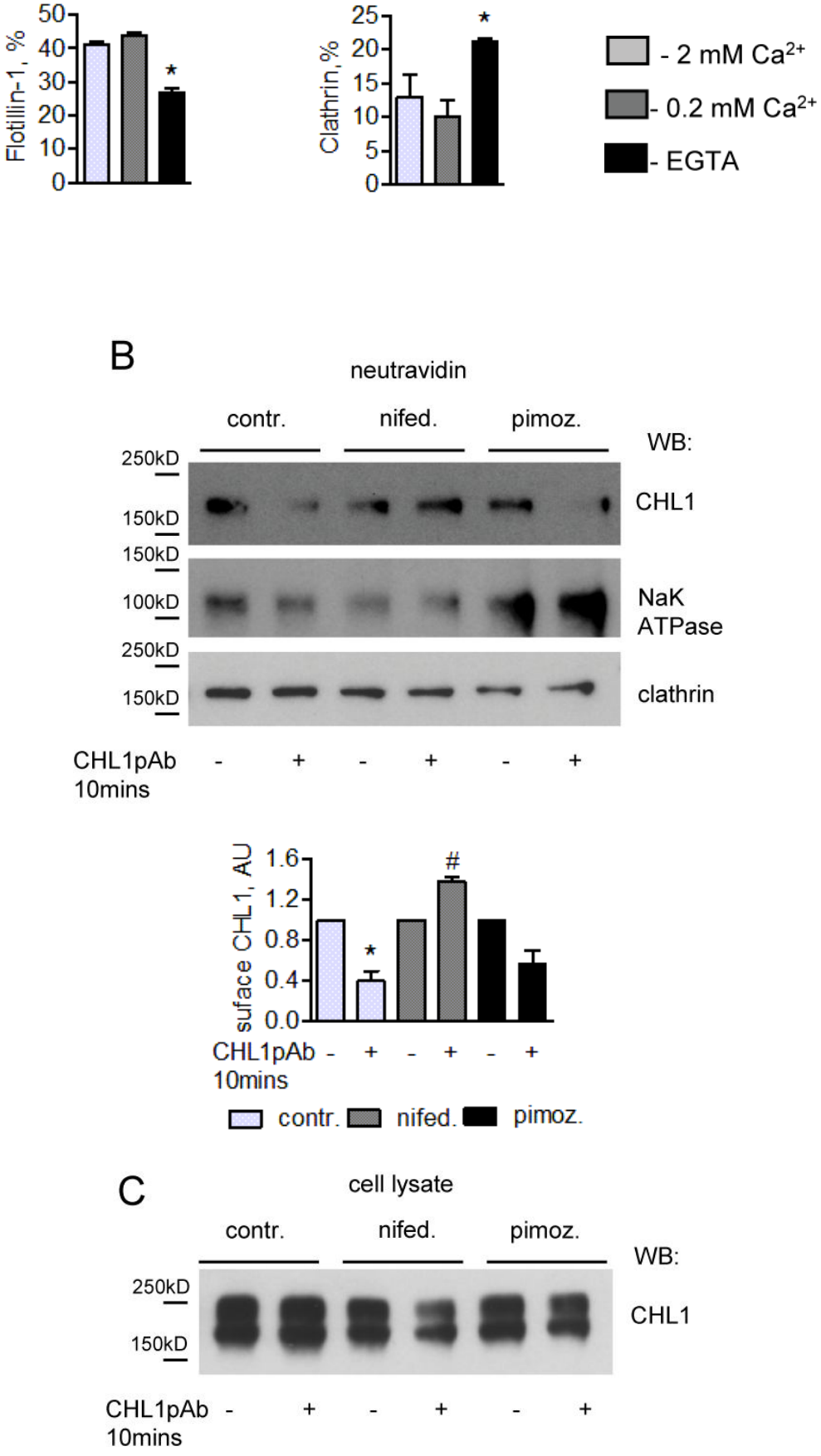

Figure VI.6. CHL1/flotillin complex formation and CHL1 endocytosis are promoted by Ca2+

(A) CHL1 was immunoprecipitated from membrane fractions of CHL1+/+ mice in the presence of 2mM Ca^{2+}, 0.2mM Ca^{2+} or 2mM EGTA. Input material and precipitates were analyzed by Western blot (WB) as indicated. Note that Ca^{2+} inhibits the co-immunoprecipitation of βII spectrin, AP2 and clathrin, and promotes the co-immunoprecipitation of flotillin-1 with CHL1. Graphs show quantitation of blots (mean values ± SEM, n=3) with the levels of the co-immunoprecipitated proteins normalized to the total levels of these proteins in the input material . *, $P < 0.05$, *t* test. (B-C) NIH 3T3 cells transfected with CHL1WT were treated with CHL1 antibodies in the presence or absence of VDCC inhibitors nifedipine or pimozide. Surface proteins were then biotinylated and immunoprecipitated from cell lysates with neutravidin agarose beads. Lysates (C) and precipitates (B) were analyzed by Western blot (WB) as indicated. Graph (B) shows quantitation of blots (mean values ± SEM, n=3). Note that nifedipine, but pimozide inhibits CHL1 antibody-induced removal of CHL1 from the cell surface. Na,K-ATPase and clathrin were used as loading control. The overall CHL1 expression in cell lysates is not affected by CHL1 antibodies and VDCC inhibitors (C). *, $P < 0.05$, paired t test.

VI.7 The association of CHL1 with lipid rafts is important for CHL1-dependent neurite outgrowth

Since clustering of CHL1 at the cell surface induces lipid raft-dependent CHL1 internalization and CHL1-mediated βII cytoskeleton remodeling, we investigated whether CHL1-dependent neurite outgrowth, which is also induced in response to the clustering of CHL1 at the neuronal cell surface, depends on lipid rafts. Cultured hippocampal CHL1+/+ neurons were treated for 24 h with CHL1 antibodies or non-specific control immunoglobulins applied in the culture medium either in the presence or absence of inhibitors of cholesterol or sphingolipid biosynthesis, to inhibit lipid raft assembly. The analysis of the microscopic images of these neurons showed that neurons treated with CHL1 antibodies in the absence of inhibitors had approximately 30% longer putative axons, identified as longest neurites, when compared with control neurons incubated with non-specific IgG. (Fig.VI.7A). However, this CHL1-dependent increase in neurite lengths was blocked by mevinolin, an inhibitor of cholesterol synthesis, fumonisin B, a fungal metabolite that inhibits biosynthesis of sphingolipids, or *N*-butyldeoxynojirimycin (NB-DNJ), a blocker of glycosphingolipid synthesis (Fig. VI.7). The inhibitors had no effects on the basal neurite outgrowth in neurons incubated with control IgG (Fig. VI.7A).

Taken collectively, these results indicate that lipid raft integrity is important for CHL1-dependent neurite outgrowth.

We then asked whether the palmitoylation-dependent targeting of CHL1 to lipid rafts is required for the CHL1-mediated neurite outgrowth. Cultured hippocampal CHL1+/+ neurons were transfected with the cherry fluorescent protein (ChFP) alone or cherry together with CHL1WT or CHL1C1102S. Exposure of ChFP only-transfected neurons to CHL1 antibodies applied in the culture medium resulted in an approximately 30% increase in the length of longest neurites, considered as putative axons, when compared to non-specific immunoglobulin treated ChFP-transfected neurons (Fig. VI.7B). An even stronger effect was observed when total neurite length of all neurites per neuron was analyzed (Fig. VI.7B). The basal neurite outgrowth in neurons co-transfected with ChFP together with CHL1WT was reduced when compared to ChFP only transfected neurons (Fig. VI.7B). This observation is in agreement with our previous data showing that increased CHL1-mediated adhesion may have an inhibitory effect on neurite outgrowth (Jakovcevski et al., 2007). However, application of CHL1 antibodies to CHL1WT co-transfected neurons elicits an increase in neurite lengths similar to that in ChFP only-transfected neurons (Fig. VI.7B). In contrast, the ability of neurons to respond to CHL1 antibodies was strongly inhibited in neurons co-transfected with ChFP together with CHL1C1102S (Fig. VI.7B). This observation indicates that the association of CHL1 with lipid rafts is required for CHL1-dependent neurite outgrowth

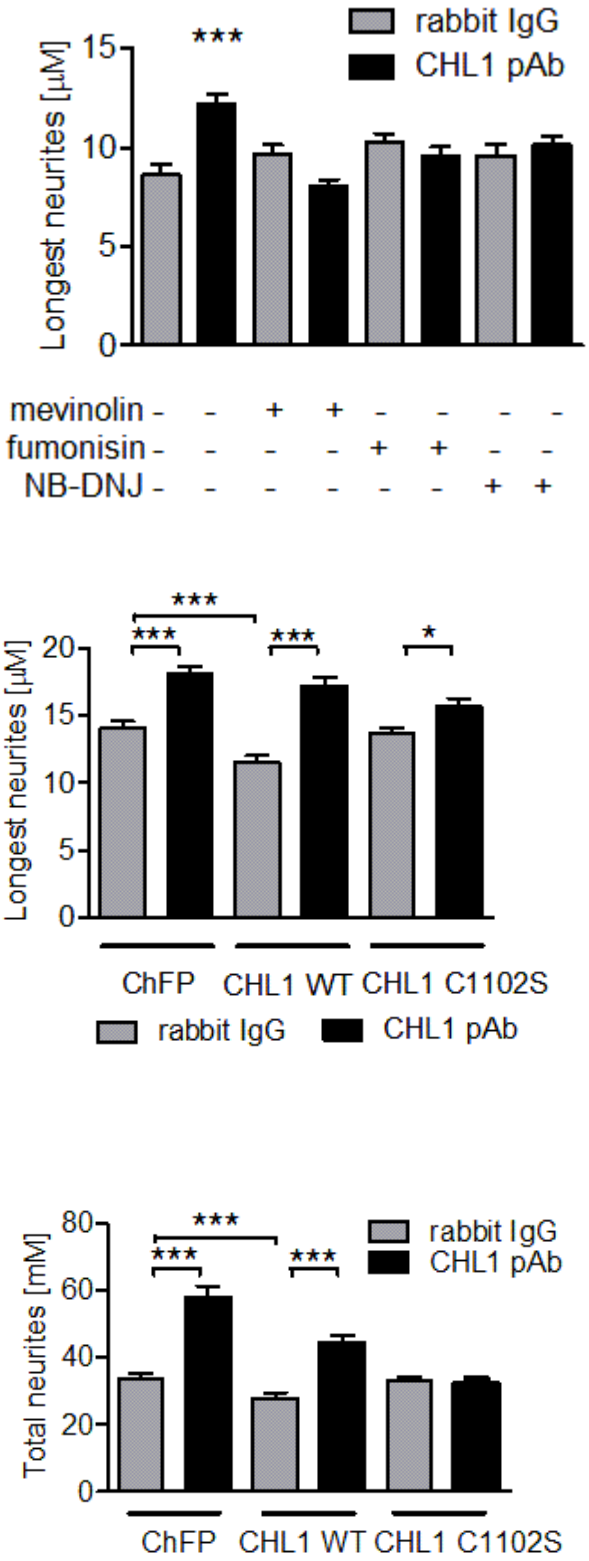

Figure.VI.7. CHL1 dependent neurite outgrowth depends on the association of CHL1 with lipid rafts.

(A) CHL1+/+ cultured hippocampal neurons were treated for 24 h with non specific immunoglobulins (IgG) or CHL1 antibodies (CHL1pAb) in the presence or absence of fumonisin B, an inhibitor of sphingomyelin and glycosphingolipid biosynthesis, N-butyldeoxynojirimycin (NB-DNJ), a blocker of glycosphingolipid

biosynthesis, or mevinolin, an inhibitor of cholesterol biosynthesis. Graph shows lengths of the longest neurites of the neurons (mean values ± SEM, n > 100). Note that all three inhibitors inhibit CHL1-dependent neurite outgrowth. (B) Cultured hippocampal neurons transfected with cherry, or co-transfected with cherry together with CHL1WT or CHL1C1102S were treated with non specific IgG or CHL1 antibodies for 24 h. Graphs show lengths of the longest neurites (upper graph) or all neurites (lower graph) of the neurons (mean values ± SEM, n > 250). Note that over-expression of CHL1C1102S inhibits the response to CHL1 antibodies. Over-expression of CHL1WT reduces overall neurite outgrowth but does not block the ability of neurons to respond to CHL1 antibodies. *, $P < 0.05$; **, $P < 0.01$; ***, $P < 0.001$, *t* test.

VII DISCUSSION

Molecules of L1 family share the high similarity in structure features and contribute to certain common fuctional events, like neurite outgrowth, axon guidance, neuronal migration (Maness and Schachner, 2007). Addressing specific roles of each molecule will help us to understand the complexity and precision in the regulation of nervous system development. As the latest member of L1 family, CHL1 attracts lots of interests due to its unique features. In cerebral cortex, unlike the uniformly-distributed L1, CHL1 is expressed in a gradient in pyramidal neurons during brain development (Demyanenko et al., 2004). During cerebellum formation, CHL1 is expressed by both neuron and Bergmann glial cells, and helps in the interaction between neuron and glia which is essential for proper axon projection (Ango et al., 2008). In a synapse, CHL1 plays a special role in vesicle recycling by regulating uncoating of clathrin-coated vesicles (Leshchyns'ka et al., 2006). An unexpected better functional recovery of CHL1-deficient mice after spinal cord injury forces people to reconsider the role of CHL1 in neurite outgrowth (Jakovcevski et al., 2007).

The present work demonstrates a novel mechanism underlying CHL1 -mediated neurite outgrowth: the internalization of CHL1 plays an important role in regulating βII spectrin and promoting neurite outgrowth in a lipid rafts -dependent manner. This study establishes a direct structural and functional connection between βII spectrin and CHL1. The interaction between CHL1 and βII spectrin is crucial for recruiting βII spectrin to lipid rafts microdomains in growth cones. CHL1 antibody-treatment induces Ca^{2+} influx via L-type VDCCs, which dissociates the CHL1-spectrin complex. As a consequence, spectrin is detached from the plasma membrane, which facilitates the internalization of CHL1. Furthermore, the internalization of CHL1 depends on

its localization to lipid rafts. Finally, the dynamic association between CHL1 and βII spectrin contributes to CHL1-mediated neurite outgrowth in a lipid rafts-dependent manner.

VII.1 CHL1 associates with βII spectrin independently of ankyrin-B

CHL1 is a unique member of the L1 family containing an altered sequence in the highly conserved ankyrin-binding motif (FIGAY instead of FIGQY) within its intracellular domain. By interating with ankyrin, L1 molecules couple to spectrin membrane skeleton and contribute to stabilizing axonal membrane (Maness and Schachner, 2007). Phosphorylation of the tyrosine residue of the FIGQY motif regulates ankyrin binding (Jenkins et al., 2001). Whether the non-conserved ankyrin-binding motif in the CHL1 ID still mediates the anykrin-CHL1 interaction was the first question we needed to answer. The present results showed that, like other L1 molecules, CHL1 forms a complex with ankyrin-B and βII spectrin in new-born mice brains illustrated by co-immunoprecipitation assay which is regarded to reflect a physiological interaction. Furthermore, the interaction between ankyrin-B and CHL1 is impaired in the presence of a tyrosine phosphatase inhibitor (vanadate) indicating a regulatory role of the tyrosine residue phosphorylation. These results are consisten with a previous study, which showed transient co-expression of CHL1 and ankyrin-G in HEK 293 cells (Human Embryonic Kidney 293 cells) recruited ankyrin from the cytosol to the cell membrane, but mutation of the tyrosine residue in the anykrin binding motif of CHL1 failed to recruit ankyrin to the plasma membrane. However, to our surprise, the association between CHL1 and βII spectrin was not changed when the amount of ankyrin-B was reduced in the CHL1-immunoprecipitaes in present of vanadate. This result indicates CHL1 directly binds βII spectrin, which we

further confirmed by ELISA assay. To our knowledge, CHL1 is the first member of L1 family identified that directly interacts with βII spectrin.

Association between CHL1 and the ankyrin/spectrin based cytoskeleton may provide CHL1 a chance to cooperate with different receptors or channels, which directly bind to ankyrin/spectrin, such as Na^+ channel, L1-CAMs, glutamate transporter EAAT4, *etc.* (Bennett and Healy, 2008). At the initial segments in neurons where action potentials are generated, neurofascin interacts with Na^+ channel by connecting with ankyrin-G. However, less is known about whether CAMs also help to organize functional domains in special area. The present data showed that ankyrin-B and βII spectrin levels were decreased in growth cones isolated from CHL1-/- mice brains, suggesting a role of CHL1 in targeting these proteins to special areas, such as the growth cone, while total levels of ankyrin-B and βII spectrin were increased. It is not yet known whether a feed-back signaling pathway is implicated in this process. Loss of spectrin in growth cones may result in unstable synapse formation later on (Pielage et al., 2005). This is consistent with the impairment in hippocampal synaptic transmission observed in CHL1 -/- mice (Nikonenko et al., 2006). Interestingly, both CHL1 and βII spectrin are important for repulsion guidance for axon growth (Garbe et al., 2007; Czogalla and Sikorski, 2005; Schlatter et al., 2008; Wright et al., 2007). Whether the decrease in βII spectrin in CHL1-/- growth cones contributes to the misguidance of axons observed in CHL1 -/- mice will reguire further study.

VII.2 CHL1 plays a role in recruiting βII spectrin to lipid rafts

Lipid-rafts are hypothetical microdomains in plasma membrane, which enriched in cholesterol and sphingolipids. Lots of interesting features about lipid rafts have been discovered since it was first proposed by Simons & Ikonen in 1997 (Simons and Ikonen, 1997). Now lipid rafts are thought to be

involved in many cellular functions, in particular, signal transduction (Golub et al., 2004). Many CAMs are present in lipid rafts, like L1 and NCAM (Olive et al., 1995; Niethammer et al., 2002). We found CHL1 was also present in isolated lipid rafts fractions, which were extracted from total membrane fractions using non-ironic detergent (Triton X-100) on ice, a classic method to study lipid-rafts associated proteins. Lipid rafts are considered as platforms to organize different molecules involving in specialized signaling transductions. L1 has been shown to form a complex with F3/contractin, a glycosylphosphatidylinositol (GPI)-linked CAM, which may contribute to the activate src family tyrosine kinase (Loers et al., 2005; Crossin and Krushel, 2000). Recently, CHL1 was shown to associate with NB-3 which belongs to F3/contatin family, and regulate the activity of tyrosine phosphatase α (PTPα). Association with GPI-linked proteins may help CHL1 participate in lipid rafts.

Lipid rafts are also important for cytoskeletal rearrangement. It has been shown that activation of NCAM enhances the formation of NCAM-spectrin complexes and results in their redistribution to lipid-rafts (Leshchyns'ka et al., 2003). The present results showed that association of βII spectrin with lipid rafts was decreased in CHL1-/- mice, suggesting a role for CHL1 in targeting βII spectrin to lipid rafts. Furthermore, mutation of the palmitoylation site within the CHL1 ID reduced its capacity to associate with lipid rafts. Replacement of the cysteine residue with a serine is a useful tool to inhibit raft localization of proteins (Zhang et al., 1998). As expected, the cysteine-to-serine mutation of CHL1 reduced βII spectrin levels in lipid rafts fractions, which confirmed CHL1 in recruiting βII spectrin to lipid rafts. Furthermore, recruitment of βII spectrin to lipid rafts by CHL1 may be independent of ankyrin-B, for the levels of ankyrin-B in lipid-rafts were increased in CHL1-/- mice. A potential lipid-binding activity found in ankyrin-binding domain of spectrin suggests that the translocation of spectrin to lipid-rafts may accompany with dissociation between spectrin and ankyrin (Bok et al., 2007). However, little is known

about this point. Another explanation for the increased amount of ankyrin in lipid-rafts of CHL1-/- mice simply might be due to the increased amount of ankyrin in total brain homogenates, which also suggested CHL1 is not necessary for the lipid-rafts localization of ankyrin. Whether the palmitoylation of CHL1 is induced by activation of CHL1 needs to be demonstrated by further experiments.

VII.3 CHL1 is involved in remodeling of spectrin mesh-work in a lipid rafts-dependent manner

CAMs mediate not only static cell-cell adhesion, but also temporally and spatially-regulated signals required for brain development. Therefore, the amount and distribution of CAMs on the cell surface should be effectively regulated in response to external stimuli during neurite outgrowth and guidance. Such regulation of CAMs can be achieved via distinct mechanisms: CAM trafficking, proteolytic cleavage of the CAM ectodomain and transcriptional regulation of CAM expression (Kamiguchi and Lemmon, 2000a). The present results showed a fast decrease in CHL1 from the cell surface triggered by CHL1 antibodies application. In this case, the total amount of CHL1 was not significantly changed, which may exclude the possibilities of proteolytic and transcriptional regulation. We hypothesize that CHL1 is internalized upon CHL1 antibody application into the live cells. Endocytosis is an important way to regulate the surface localization of CAMs. However, after clustering CHL1 by antibodies, what kind of signals could be active to trigger endocytosis? It has been shown that clustering L1 and NCAM by antibodies both induces Ca^{2+} influx via VDCC (Williams et al., 1992b; Niethammer et al., 2002). In present study, the inhibitors of L-type, but not T-type VDCC, blocked internalization of CHL1 induced by CHL1 antibody application, indicating Ca^{2+} influx via L-type VDCC is important for CHL1

internalization. Ca^{2+} influx after clustering CAMs may play a general role in CAM-related signalings. Since VDCC is enriched in lipid rafts microdomains (Bodrikov et al., 2008), we were interested in investigating whether localization of CHL1 in lipid rafts was necessary for its internalization. The mutation of CHL1 at the palmitoylation site, which reduced the capacity of CHL1 to associate with lipid rafts, stabilized CHL1 cell surface levels after clustering CHL1 for 10 min. We also noticed a variable reduction of mutant CHL1 from cell surface after a prolonged stimulation (unpublished data), which indicated the existence of different regulation mechanisms in different time courses.

In present study, we also observed that clustering of CHL1 induced detachment of βII spectrin from the plasma membrane. We speculate that the influx of Ca^{2+} may result in partially dissociation of spectrin mesh-work facilitating the followed endocytosis of CHL1. This speculation is based on the facts that spectrin mesh-work could be dissociated by calpain, a calcium-dependent protease, and loss of spectrin from the membrane has been previously observed at the final stage of clathrin-mediated endocytosis (Kamal et al., 1998; Harris and Morrow, 1990; Gerke and Moss, 1997; Czogalla and Sikorski, 2005). Furthermore, our results showed that the association between CHL1 and βII spectrin was dramatically reduced after CHL1 antibodies application, suggesting a specific role of CHL1 in regulating the spectrin cytoskeleton. This point was also confirmed by evidence that the association between CHL1 and βII spectrin was inversely related to calcium concentration. In agreement with the above results, we also noticed that polymerized spectrin levels were increased in CHL1-/- mice brains. Taken together, these results suggest CHL1 plays a role in remodeling the spectrin mesh-work.

The next question raised from these results is which specific endocytic

pathway mediates the internalization of CHL1. The best characterized endocytic pathway is the clathrin-dependent pathway by which most membrane proteins undergo endocytosis (Mousavi et al., 2004). The L1 cytoplasmic domain carries the endocytic motif recognized by the clathrin-associated adaptor protein AP2. Moreover, the L1-based neurite growth is positively related to the amount of endocytosed L1 in the growth cone (Kamiguchi and Yoshihara, 2001). Although CHL1 has no conserved AP2 binding motif in the cytoplasmic domain, it still could be endocytosed by the clathrin-mediated pathway in response to synapse activation and help uncoating of clathrin coated vesicles (Leshchyns'ka et al., 2006). Indeed, we also found CHL1 associated with clathrin and AP2 in young mice brains by coimmunoprecipitation in absence of Ca^{2+}. However, this complex dissociatesd when Ca^{2+} concentrations increase, which indicated an alternative endocytic pathway may mediate internalization of CHL1 triggered by Ca^{2+} influx. Since the internalization of CHL1 was dependent on its lipid-rafts localization, the lipid rafts marker, flotillin-1/reggie-2-mediated endocytic pathway is the most likely candidate (Langhorst et al., 2005). Compared with caveolin, another lipid rafts marker, that is less abundant in the brain, flotillin-1/reggie-2 is highly expressed in brain and spinal cord (Lang et al., 1998). Moreover, like CHL1, flotillin-1/reggie-2 is strongly up-regulated during axon regeneration (Schulte et al., 1997; Chaisuksunt et al., 2000). Indeed, present results showed CHL1 could coimmunoprecipitate with flotillin-1/reggie-2 in young mice brains, and this association was enhanced in presence of Ca^{2+}. This indicates that the endocytosis of CHL1 might be mediated by the flotillin-1/reggie-2 pathway. A more detailed investigation is required to characterize the role of flotillin-1/reggie-2 in the endocytosis of CHL1.

VII.4 Lipid rafts are important for CHL1-mediated neurite outgrowth

Several studies have underlined the importance of CHL1 in axon guidance and dendritic orientation during brain development (Demyanenko et al., 2004; Heyden et al., 2008; Ango et al., 2008; Montag-Sallaz et al., 2002; Ye et al., 2008; Schlatter et al., 2008; Wright et al., 2007). However, the exact role of CHL1 in neurite outgrowth is still ambiguous. Some studies propose CHL1 promotes neurite outgrowth through heterophilic interaction with an unknown binding partner, probably βI Integrin (Buhusi et al., 2003; Hillenbrand et al., 1999b; Schlatter et al., 2008). Whereas a contradictory study suggests that loss of hemophilic CHL1 binding between neurons and astrocytes which inhibits neurite outgrowth, resultes in better functional recovery after spinal cord injury (Jakovcevski et al., 2007). Thus a dual functional hypothesis of CHL1 underlying neurite outgrowth was proposed by Jakovcevski *et al.*: CHL1 could promote neurite by its heterophilic interaction but inhibit neurite outgrowth by its homophilic interaction (Jakovcevski et al., 2007). However, the mechanism of CHL1-mediated neurite outgrowth based on this hypothesis is still unknown.

In the present study, cultured hippocampal neurons extended longer neurite in the presence of CHL1-specific antibodies in the culture media compared to non-specific rabbit IgG. According to our findings in fibroblasts, the endocytosis of CHL1 can be induced by CHL1 antibodies application. Thus, we hypothesize that the endocytosis of CHL1 may contribute to promoting neurite outgrowth. While antibodies may perturb CHL1 homophilic binding between neighbouring cells, such as disruption may mimic CHL1 endocytosis needed for proper neurite outgrowth. For example, after spinal cord injury, the strong interaction between neurons and astrocytes mediated by CHL1

homophilic binding plays a negative role in axon regeneration (Jakovcevski et al., 2007). Ectodomain shedding of CHL1 by ADAM8 induces a more vigorous neurite outgrowth and may provide indirect evidence for the inhibitory role of CHL1 homophilic binding in neurite outgrowth (Naus et al., 2004). At the same time, proper interaction between neuron and glia mediated by CHL1 is necessary as observed for proper axon projection during mice cerebellum development (Ango et al., 2008).

Interestingly, our results showed that lipid rafts were important for neurite outgrowth induced by CHL1 antibodies application. The first clue was based on experiments using pharmacological agents that disrupt lipid rafts blocked neurite outgrowth induced by CHL1 antibodies application. This result indicates the integrity of lipid rafts is necessary for CHL1-dependent neurite outgrowth. It is less likely that the inhibitors has a general effect on neurite outgrowth inhibition, because the neurite lengths of neurons incubated with non-specific rabbit IgG was not significantly influenced by identical treatment with inhibitors. It has been reported that the lipid rafts are also important for L1 but not β1 integrin-mediated neurite growth, because L1 is localized in lipid rafts but β1 integrin is exclusively localized outside lipid rafts (Nakai and Kamiguchi, 2002). These conclusions are consistent with our present results, as we found CHL1 was also in lipid rafts. So we further speculate that the CHL1-mediated neurite outgrowth through lipid rafts is independent of β1 integrin, a known binding partner of CHL1 (Buhusi et al., 2003).

Since the mutation in the palmityolation site of CHL1 ID (C1102S) reduced its capacity to associate with lipid rafts. Overexpression of this mutant CHL1 in neurons abolished the promotion effects of neurite outgrowth induced by CHL1 specific antibodies, strongly suggesting that lipid rafts localization of CHL1 is indeed necessary for CHL1-mediated neurite outgrowth. Considering that this mutation stabilized CHL1 at cell surface in response to CHL1

clustering, this result again confirmed our hypothesis that endocytosis of CHL1 is an important factor in CHL1-mediated neurite outgrowth.

To summarized our results, we propose the following working model for CHL1-mediated neurite outgrowth: CHL1 interacts with βII spectrin and recruits it to lipid raft in growth cone; clustering of CHL1 on cell surface induces more relocalization of CHL1-βII spectrin complexes lipid rafts and induces Ca^{2+} influx into the cell via L-type calcium channel; as a consequence, detachment of βII spectrin from plasma membrane facilitates the endocytosis of CHL1, which contributes to proper neurite outgrowth (Fig. VII.1.).

In conclusion, we provide a novel mechanism underlying CHL1-mediated neurite outgrowth by which the spatial regulation of CHL1 together with βII spectrin is largely dependent on lipid rafts. Our study emphasizes the importance of CHL1 on proper neurite outgrowth which may further correlates with the proper synaptic formation during brain development. Considering that the CHL1 gene is implied in metal retardation and schizophrenia (Frints et al., 2003; Angeloni et al., 1999a; Sakurai et al., 2002), a better understanding of CHL1-mediated neurite outgrowth may help us to understand the etiology of these disease.

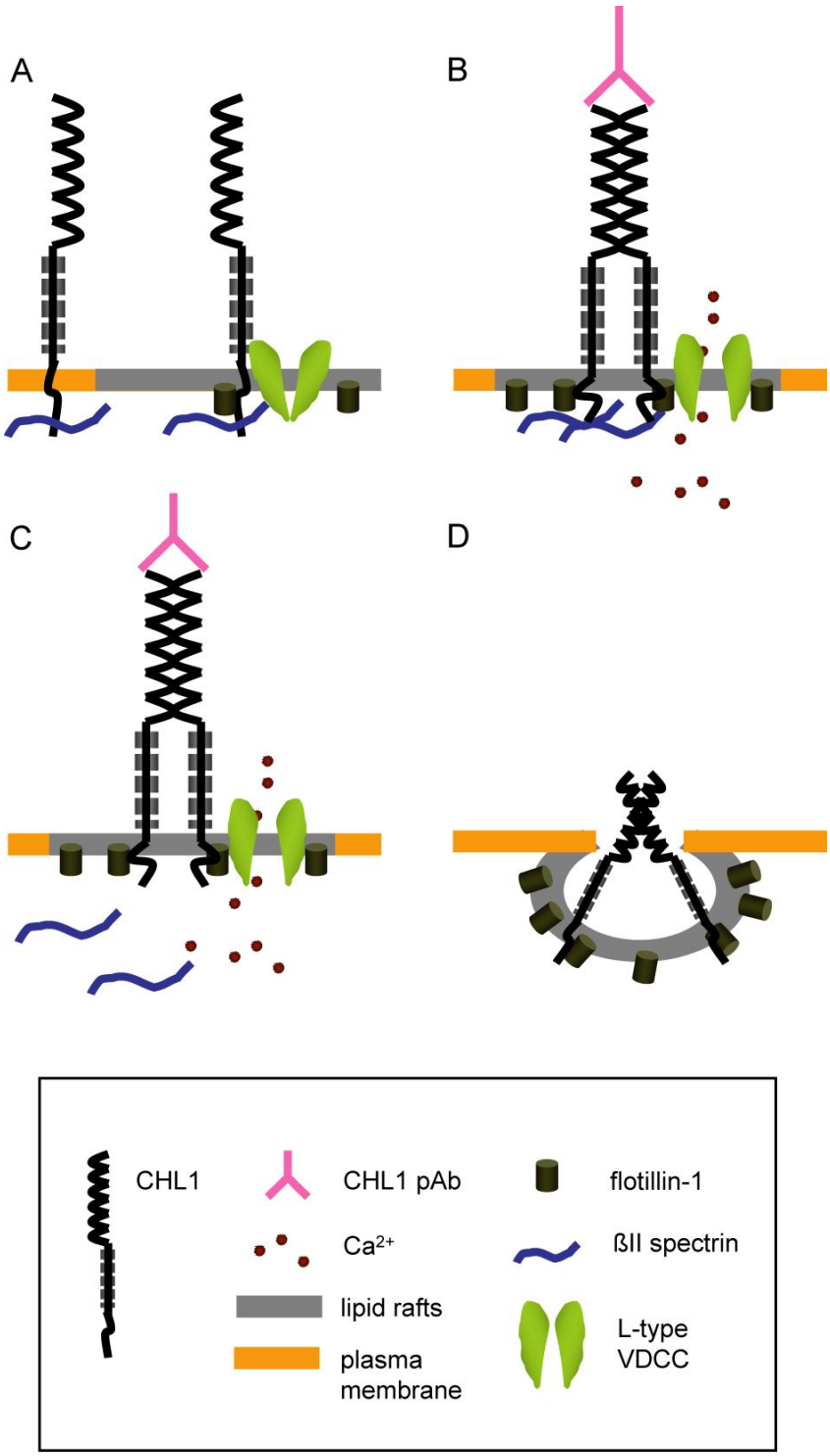

Figure VII.1. Proposed model illustrating the dynamic regulation of βII spectrin by CHL1.

(A) CHL1 interacts with βII spectrin and recruits it to lipid raft in growth cone;

(B) Clustering of CHL1 on cell surface induces more CHL1-βII spectrin complexes relocalization to lipid rafts and influx of Ca2+ into the cell via L-type calcium channel;

(C)-(D) As a consequence, detachment of βII spectrin from plasma membrane facilitates the endocytosis of CHL1 , which contributes to a proper neurite outgrowth.

VIII REFERENCES

Aksana Andreyeva. Neural recognition molecule CHL1: regulation of the activity of the trimeric protein complex Csp/Hsc70/Sgt and synaptic vesicle recycling . 2008.

Ref Type: Thesis/Dissertation

Angeloni,D., Lindor,N.M., Pack,S., Latif,F., Wei,M.H., and Lerman,M.I. (1999a). CALL gene is haploinsufficient in a 3p- syndrome patient. Am. J. Med. Genet. *86*, 482-485.

Angeloni,D., Wei,M.H., and Lerman,M.I. (1999b). Two single nucleotide polymorphisms (SNPs) in the CALL gene for association studies with IQ. Psychiatr. Genet. *9*, 165-167.

Ango,F., Wu,C., Van der Want,J.J., Wu,P., Schachner,M., and Huang,Z.J. (2008). Bergmann glia and the recognition molecule CHL1 organize GABAergic axons and direct innervation of Purkinje cell dendrites. PLoS Biol. *6*, e103.

Archer,F.R., Doherty,P., Collins,D., and Bolsover,S.R. (1999). CAMs and FGF cause a local submembrane calcium signal promoting axon outgrowth without a rise in bulk calcium concentration. Eur. J. Neurosci. *11*, 3565-3573.

Barclay,A.N. (2003). Membrane proteins with immunoglobulin-like domains--a master superfamily of interaction molecules. Semin. Immunol. *15*, 215-223.

Barreiro,O., Yanez-Mo,M., Serrador,J.M., Montoya,M.C., Vicente-Manzanares,M., Tejedor,R., Furthmayr,H., and Sanchez-Madrid,F. (2002). Dynamic interaction of VCAM-1 and ICAM-1 with moesin and ezrin in a novel endothelial docking structure for adherent leukocytes. J. Cell Biol. *157*, 1233-1245.

Basu,J. (2004). Protein palmitoylation and dynamic modulation of protein function. Current Science *87*, 212-217.

Bennett,V. and Baines,A.J. (2001). Spectrin and ankyrin-based pathways: metazoan inventions for integrating cells into tissues. Physiol Rev. *81*, 1353-1392.

Bennett,V. and Healy,J. (2008). Organizing the fluid membrane bilayer:

diseases linked to spectrin and ankyrin. Trends Mol. Med. *14*, 28-36.

Bodrikov,V., Leshchyns'ka,I., Sytnyk,V., Overvoorde,J., den Hertog,J., and Schachner,M. (2005). RPTPalpha is essential for NCAM-mediated p59fyn activation and neurite elongation. J. Cell Biol. *168*, 127-139.

Bodrikov,V., Sytnyk,V., Leshchyns'ka,I., den Hertog,J., and Schachner,M. (2008). NCAM induces CaMKIIalpha-mediated RPTPalpha phosphorylation to enhance its catalytic activity and neurite outgrowth. J. Cell Biol. *182*, 1185-1200.

Bok,E., Plazuk,E., Hryniewicz-Jankowska,A., Chorzalska,A., Szmaj,A., Dubielecka,P.M., Stebelska,K., Diakowski,W., Lisowski,M., Langner,M., and Sikorski,A.F. (2007). Lipid-binding role of betaII-spectrin ankyrin-binding domain. Cell Biol. Int. *31*, 1482-1494.

Bretscher,A., Edwards,K., and Fehon,R.G. (2002). ERM proteins and merlin: integrators at the cell cortex. Nat. Rev. Mol. Cell Biol. *3*, 586-599.

Brummendorf,T. and Rathjen,F.G. (1994). Cell adhesion molecules. 1: immunoglobulin superfamily. Protein Profile. *1*, 951-1058.

Buhusi,M., Midkiff,B.R., Gates,A.M., Richter,M., Schachner,M., and Maness,P.F. (2003). Close homolog of L1 is an enhancer of integrin-mediated cell migration. J. Biol. Chem. *278*, 25024-25031.

Castellani,V., De Angelis,E., Kenwrick,S., and Rougon,G. (2002). Cis and trans interactions of L1 with neuropilin-1 control axonal responses to semaphorin 3A. EMBO J. *21*, 6348-6357.

Castellani,V., Falk,J., and Rougon,G. (2004). Semaphorin3A-induced receptor endocytosis during axon guidance responses is mediated by L1 CAM. Mol. Cell Neurosci. *26*, 89-100.

Chaisuksunt,V., Campbell,G., Zhang,Y., Schachner,M., Lieberman,A.R., and Anderson,P.N. (2000). The cell recognition molecule CHL1 is strongly upregulated by injured and regenerating thalamic neurons. J. Comp Neurol. *425*, 382-392.

Chen,Q.Y., Chen,Q., Feng,G.Y., Lindpaintner,K., Chen,Y., Sun,X., Chen,Z., Gao,Z., Tang,J., and He,L. (2005). Case-control association study of the close homologue of L1 (CHL1) gene and schizophrenia in the Chinese population. Schizophr. Res. *73*, 269-274.

Cheng,L., Itoh,K., and Lemmon,V. (2005). L1-mediated branching is regulated by two ezrin-radixin-moesin (ERM)-binding sites, the RSLE region and a novel juxtamembrane ERM-binding region. J. Neurosci. *25*, 395-403.

Crossin,K.L. and Krushel,L.A. (2000). Cellular signaling by neural cell adhesion molecules of the immunoglobulin superfamily. Dev. Dyn. *218*, 260-279.

Czogalla,A. and Sikorski,A.F. (2005). Spectrin and calpain: a 'target' and a 'sniper' in the pathology of neuronal cells. Cell Mol. Life Sci. *62*, 1913-1924.

Davis,J.Q. and Bennett,V. (1993). Ankyrin-binding activity of nervous system cell adhesion molecules expressed in adult brain. J. Cell Sci. Suppl *17*, 109-117.

Demyanenko,G.P., Schachner,M., Anton,E., Schmid,R., Feng,G., Sanes,J., and Maness,P.F. (2004). Close homolog of L1 modulates area-specific neuronal positioning and dendrite orientation in the cerebral cortex. Neuron *44*, 423-437.

Denda,S. and Reichardt,L.F. (2007). Studies on integrins in the nervous system. Methods Enzymol. *426*, 203-221.

Dent,E.W. and Gertler,F.B. (2003). Cytoskeletal dynamics and transport in growth cone motility and axon guidance. Neuron *40*, 209-227.

Diestel,S., Schaefer,D., Cremer,H., and Schmitz,B. (2007). NCAM is ubiquitylated, endocytosed and recycled in neurons. J. Cell Sci. *120*, 4035-4049.

Doherty,P., Williams,G., and Williams,E.J. (2000). CAMs and axonal growth: a critical evaluation of the role of calcium and the MAPK cascade. Mol. Cell Neurosci. *16*, 283-295.

Dubreuil,R.R., Byers,T.J., Sillman,A.L., Barzvi,D., Goldstein,L.S.B., and Branton,D. (1989). The Complete Sequence of Drosophila Alpha-Spectrin - Conservation of Structural Domains Between Alpha-Spectrins and Alpha-Actinin. Journal of Cell Biology *109*, 2197-2205.

Fan,J., Mansfield,S.G., Redmond,T., Gordon-Weeks,P.R., and Raper,J.A. (1993). The organization of F-actin and microtubules in growth cones exposed to a brain-derived collapsing factor. J. Cell Biol. *121*, 867-878.

Fransen,E., Lemmon,V., Van Camp,G., Vits,L., Coucke,P., and Willems,P.J.

(1995). CRASH syndrome: clinical spectrum of corpus callosum hypoplasia, retardation, adducted thumbs, spastic paraparesis and hydrocephalus due to mutations in one single gene, L1. Eur. J. Hum. Genet. *3*, 273-284.

Frints,S.G., Marynen,P., Hartmann,D., Fryns,J.P., Steyaert,J., Schachner,M., Rolf,B., Craessaerts,K., Snellinx,A., Hollanders,K., D'Hooge,R., De Deyn,P.P., and Froyen,G. (2003). CALL interrupted in a patient with non-specific mental retardation: gene dosage-dependent alteration of murine brain development and behavior. Hum. Mol. Genet. *12*, 1463-1474.

Fulga,T.A. and Van Vactor,D. (2008). Synapses and growth cones on two sides of a highwire. Neuron *57*, 339-344.

Garbe,D.S., Das,A., Dubreuil,R.R., and Bashaw,G.J. (2007). beta-Spectrin functions independently of Ankyrin to regulate the establishment and maintenance of axon connections in the Drosophila embryonic CNS. Development *134*, 273-284.

Garver,T.D., Ren,Q., Tuvia,S., and Bennett,V. (1997). Tyrosine phosphorylation at a site highly conserved in the L1 family of cell adhesion molecules abolishes ankyrin binding and increases lateral mobility of neurofascin. J. Cell Biol. *137*, 703-714.

Gerke,V. and Moss,S.E. (1997). Annexins and membrane dynamics. Biochim. Biophys. Acta *1357*, 129-154.

Glebov,O.O., Bright,N.A., and Nichols,B.J. (2006). Flotillin-1 defines a clathrin-independent endocytic pathway in mammalian cells. Nat. Cell Biol. *8*, 46-54.

Goldberg,D.J. and Burmeister,D.W. (1986). Stages in axon formation: observations of growth of Aplysia axons in culture using video-enhanced contrast-differential interference contrast microscopy. J. Cell Biol. *103*, 1921-1931.

Goldberg,J.L. (2004). Intrinsic neuronal regulation of axon and dendrite growth. Curr. Opin. Neurobiol. *14*, 551-557.

Golub,T., Wacha,S., and Caroni,P. (2004). Spatial and temporal control of signaling through lipid rafts. Curr. Opin. Neurobiol. *14*, 542-550.

Gomez,T.M. and Zheng,J.Q. (2006). The molecular basis for calcium-dependent axon pathfinding. Nat. Rev. Neurosci. *7*, 115-125.

Grum,V.L., Li,D.N., MacDonald,R.I., and Mondragon,A. (1999). Structures of two repeats of spectrin suggest models of flexibility. Cell *98*, 523-535.

Guirland,C., Suzuki,S., Kojima,M., Lu,B., and Zheng,J.Q. (2004). Lipid rafts mediate chemotropic guidance of nerve growth cones. Neuron *42*, 51-62.

Hamada,K., Shimizu,T., Yonemura,S., Tsukita,S., Tsukita,S., and Hakoshima,T. (2003). Structural basis of adhesion-molecule recognition by ERM proteins revealed by the crystal structure of the radixin-ICAM-2 complex. EMBO J. *22*, 502-514.

Hammarlund,M., Davis,W.S., and Jorgensen,E.M. (2000). Mutations in beta-spectrin disrupt axon outgrowth and sarcomere structure. Journal of Cell Biology *149*, 931-942.

Hammarlund,M., Jorgensen,E.M., and Bastiani,M.J. (2007). Axons break in animals lacking beta-spectrin. Journal of Cell Biology *176*, 269-275.

Hardy,B., Bensch,K.G., and Schrier,S.L. (1979). Spectrin rearrangement early in erythrocyte ghost endocytosis. J. Cell Biol. *82*, 654-663.

Harper,S.J., Bolsover,S.R., Walsh,F.S., and Doherty,P. (1994). Neurite outgrowth stimulated by L1 requires calcium influx into neurons but is not associated with changes in steady state levels of calcium in growth cones. Cell Adhes. Commun. *2*, 441-453.

Harris,A.S. and Morrow,J.S. (1990). Calmodulin and calcium-dependent protease I coordinately regulate the interaction of fodrin with actin. Proc. Natl. Acad. Sci. U. S. A *87*, 3009-3013.

Henley,J. and Poo,M.M. (2004). Guiding neuronal growth cones using Ca2+ signals. Trends Cell Biol. *14*, 320-330.

Henley,J.R., Huang,K.H., Wang,D., and Poo,M.M. (2004). Calcium mediates bidirectional growth cone turning induced by myelin-associated glycoprotein. Neuron *44*, 909-916.

Heyden,A., Angenstein,F., Sallaz,M., Seidenbecher,C., and Montag,D. (2008). Abnormal axonal guidance and brain anatomy in mouse mutants for the cell recognition molecules close homolog of L1 and NgCAM-related cell adhesion molecule. Neuroscience *155*, 221-233.

Hillenbrand,R., Molthagen,M., Montag,D., and Schachner,M. (1999a). The close homologue of the neural adhesion molecule L1 (CHL1): patterns of

expression and promotion of neurite outgrowth by heterophilic interactions. Eur. J. Neurosci. *11*, 813-826.

Hillenbrand,R., Molthagen,M., Montag,D., and Schachner,M. (1999b). The close homologue of the neural adhesion molecule L1 (CHL1): patterns of expression and promotion of neurite outgrowth by heterophilic interactions. Eur. J. Neurosci. *11*, 813-826.

Holm,J., Hillenbrand,R., Steuber,V., Bartsch,U., Moos,M., Lubbert,H., Montag,D., and Schachner,M. (1996). Structural features of a close homologue of L1 (CHL1) in the mouse: a new member of the L1 family of neural recognition molecules. Eur. J. Neurosci. *8*, 1613-1629.

Hu,R.J. and Bennett,V. (1991). In vitro proteolysis of brain spectrin by calpain I inhibits association of spectrin with ankyrin-independent membrane binding site(s). J. Biol. Chem. *266*, 18200-18205.

Irintchev,A., Koch,M., Needham,L.K., Maness,P., and Schachner,M. (2004). Impairment of sensorimotor gating in mice deficient in the cell adhesion molecule L1 or its close homologue, CHL1. Brain Res. *1029*, 131-134.

Jakovcevski,I., Wu,J., Karl,N., Leshchyns'ka,I., Sytnyk,V., Chen,J., Irintchev,A., and Schachner,M. (2007). Glial scar expression of CHL1, the close homolog of the adhesion molecule L1, limits recovery after spinal cord injury. J. Neurosci. *27*, 7222-7233.

Jenkins,S.M., Kizhatil,K., Kramarcy,N.R., Sen,A., Sealock,R., and Bennett,V. (2001). FIGQY phosphorylation defines discrete populations of L1 cell adhesion molecules at sites of cell-cell contact and in migrating neurons. J. Cell Sci. *114*, 3823-3835.

Jung,N. and Haucke,V. (2007). Clathrin-mediated endocytosis at synapses. Traffic. *8*, 1129-1136.

Kamal,A., Ying,Y., and Anderson,R.G. (1998). Annexin VI-mediated loss of spectrin during coated pit budding is coupled to delivery of LDL to lysosomes. J. Cell Biol. *142*, 937-947.

Kamiguchi,H. (2006). The region-specific activities of lipid rafts during axon growth and guidance. J. Neurochem. *98*, 330-335.

Kamiguchi,H. and Lemmon,V. (2000a). IgCAMs: bidirectional signals underlying neurite growth. Curr. Opin. Cell Biol. *12*, 598-605.

Kamiguchi,H. and Lemmon,V. (2000b). Recycling of the cell adhesion molecule L1 in axonal growth cones. J. Neurosci. *20*, 3676-3686.

Kamiguchi,H., Long,K.E., Pendergast,M., Schaefer,A.W., Rapoport,I., Kirchhausen,T., and Lemmon,V. (1998). The neural cell adhesion molecule L1 interacts with the AP-2 adaptor and is endocytosed via the clathrin-mediated pathway. J. Neurosci. *18*, 5311-5321.

Kamiguchi,H. and Yoshihara,F. (2001). The role of endocytic l1 trafficking in polarized adhesion and migration of nerve growth cones. J. Neurosci. *21*, 9194-9203.

Kater,S.B., Mattson,M.P., Cohan,C., and Connor,J. (1988). Calcium regulation of the neuronal growth cone. Trends Neurosci. *11*, 315-321.

Kater,S.B. and Mills,L.R. (1991). Regulation of growth cone behavior by calcium. J. Neurosci. *11*, 891-899.

Kenwrick,S. and Doherty,P. (1998). Neural cell adhesion molecule L1: relating disease to function. Bioessays *20*, 668-675.

Kiryushko,D., Berezin,V., and Bock,E. (2004). Regulators of neurite outgrowth: role of cell adhesion molecules. Ann. N. Y. Acad. Sci. *1014*, 140-154.

Lacinova,L. (2005). Voltage-dependent calcium channels. Gen. Physiol Biophys. *24 Suppl 1*, 1-78.

Landis,D.M.D., Hall,A.K., Weinstein,L.A., and Reese,T.S. (1988). The Organization of Cytoplasm at the Presynaptic Active Zone of A Central Nervous-System Synapse. Neuron *1*, 201-209.

Lang,D.M., Lommel,S., Jung,M., Ankerhold,R., Petrausch,B., Laessing,U., Wiechers,M.F., Plattner,H., and Stuermer,C.A. (1998). Identification of reggie-1 and reggie-2 as plasmamembrane-associated proteins which cocluster with activated GPI-anchored cell adhesion molecules in non-caveolar micropatches in neurons. J. Neurobiol. *37*, 502-523.

Langhorst,M.F., Jaeger,F.A., Mueller,S., Sven,H.L., Luxenhofer,G., and Stuermer,C.A. (2008). Reggies/flotillins regulate cytoskeletal remodeling during neuronal differentiation via CAP/ponsin and Rho GTPases. Eur. J. Cell Biol. *87*, 921-931.

Langhorst,M.F., Reuter,A., and Stuermer,C.A. (2005). Scaffolding microdomains and beyond: the function of reggie/flotillin proteins. Cell Mol. Life

Sci. *62*, 2228-2240.

Leahy,D.J., Hendrickson,W.A., Aukhil,I., and Erickson,H.P. (1992). Structure of a fibronectin type III domain from tenascin phased by MAD analysis of the selenomethionyl protein. Science *258*, 987-991.

Lee,G., Abdi,K., Jiang,Y., Michaely,P., Bennett,V., and Marszalek,P.E. (2006). Nanospring behaviour of ankyrin repeats. Nature *440*, 246-249.

Leshchyns'ka,I., Sytnyk,V., Morrow,J.S., and Schachner,M. (2003). Neural cell adhesion molecule (NCAM) association with PKCbeta2 via betaI spectrin is implicated in NCAM-mediated neurite outgrowth. J. Cell Biol. *161*, 625-639.

Leshchyns'ka,I., Sytnyk,V., Richter,M., Andreyeva,A., Puchkov,D., and Schachner,M. (2006). The adhesion molecule CHL1 regulates uncoating of clathrin-coated synaptic vesicles. Neuron *52*, 1011-1025.

Letourneau,P.C., Condic,M.L., and Snow,D.M. (1994). Interactions of developing neurons with the extracellular matrix. J. Neurosci. *14*, 915-928.

Lewis,C.M., Levinson,D.F., Wise,L.H., DeLisi,L.E., Straub,R.E., Hovatta,I., Williams,N.M., Schwab,S.G., Pulver,A.E., Faraone,S.V., Brzustowicz,L.M., Kaufmann,C.A., Garver,D.L., Gurling,H.M., Lindholm,E., Coon,H., Moises,H.W., Byerley,W., Shaw,S.H., Mesen,A., Sherrington,R., O'Neill,F.A., Walsh,D., Kendler,K.S., Ekelund,J., Paunio,T., Lonnqvist,J., Peltonen,L., O'Donovan,M.C., Owen,M.J., Wildenauer,D.B., Maier,W., Nestadt,G., Blouin,J.L., Antonarakis,S.E., Mowry,B.J., Silverman,J.M., Crowe,R.R., Cloninger,C.R., Tsuang,M.T., Malaspina,D., Harkavy-Friedman,J.M., Svrakic,D.M., Bassett,A.S., Holcomb,J., Kalsi,G., McQuillin,A., Brynjolfson,J., Sigmundsson,T., Petursson,H., Jazin,E., Zoega,T., and Helgason,T. (2003). Genome scan meta-analysis of schizophrenia and bipolar disorder, part II: Schizophrenia. Am. J. Hum. Genet. *73*, 34-48.

Lin,R.C. and Scheller,R.H. (2000). Mechanisms of synaptic vesicle exocytosis. Annu. Rev. Cell Dev. Biol. *16*, 19-49.

Loers,G., Chen,S., Grumet,M., and Schachner,M. (2005). Signal transduction pathways implicated in neural recognition molecule L1 triggered neuroprotection and neuritogenesis. J. Neurochem. *92*, 1463-1476.

Main,A.L., Harvey,T.S., Baron,M., Boyd,J., and Campbell,I.D. (1992). The three-dimensional structure of the tenth type III module of fibronectin: an insight into RGD-mediated interactions. Cell *71*, 671-678.

Maness,P.F. and Schachner,M. (2007). Neural recognition molecules of the immunoglobulin superfamily: signaling transducers of axon guidance and neuronal migration. Nat. Neurosci. *10*, 19-26.

Marquardt,T., Shirasaki,R., Ghosh,S., Andrews,S.E., Carter,N., Hunter,T., and Pfaff,S.L. (2005). Coexpressed EphA receptors and ephrin-A ligands mediate opposing actions on growth cone navigation from distinct membrane domains. Cell *121*, 127-139.

Mayor,S. and Pagano,R.E. (2007). Pathways of clathrin-independent endocytosis. Nat. Rev. Mol. Cell Biol. *8*, 603-612.

Minana,R., Duran,J.M., Tomas,M., Renau-Piqueras,J., and Guerri,C. (2001). Neural cell adhesion molecule is endocytosed via a clathrin-dependent pathway. Eur. J. Neurosci. *13*, 749-756.

Molitoris,B.A., Dahl,R., and Hosford,M. (1996). Cellular ATP depletion induces disruption of the spectrin cytoskeletal network. Am. J. Physiol *271*, F790-F798.

Montag-Sallaz,M., Baarke,A., and Montag,D. (2003). Aberrant neuronal connectivity in CHL1-deficient mice is associated with altered information processing-related immediate early gene expression. J. Neurobiol. *57*, 67-80.

Montag-Sallaz,M., Schachner,M., and Montag,D. (2002). Misguided axonal projections, neural cell adhesion molecule 180 mRNA upregulation, and altered behavior in mice deficient for the close homolog of L1. Mol. Cell Biol. *22*, 7967-7981.

Mousavi,S.A., Malerod,L., Berg,T., and Kjeken,R. (2004). Clathrin-dependent endocytosis. Biochem. J. *377*, 1-16.

Nakai,Y. and Kamiguchi,H. (2002). Migration of nerve growth cones requires detergent-resistant membranes in a spatially defined and substrate-dependent manner. J. Cell Biol. *159*, 1097-1108.

Naus,S., Richter,M., Wildeboer,D., Moss,M., Schachner,M., and Bartsch,J.W. (2004). Ectodomain shedding of the neural recognition molecule CHL1 by the metalloprotease-disintegrin ADAM8 promotes neurite outgrowth and suppresses neuronal cell death. J. Biol. Chem. *279*, 16083-16090.

Niethammer,P., Delling,M., Sytnyk,V., Dityatev,A., Fukami,K., and Schachner,M. (2002). Cosignaling of NCAM via lipid rafts and the FGF receptor is required for neuritogenesis. J. Cell Biol. *157*, 521-532.

Nikonenko,A.G., Sun,M., Lepsveridze,E., Apostolova,I., Petrova,I., Irintchev,A., Dityatev,A., and Schachner,M. (2006). Enhanced perisomatic inhibition and impaired long-term potentiation in the CA1 region of juvenile CHL1-deficient mice. Eur. J. Neurosci. *23*, 1839-1852.

Ohbayashi,K., Fukura,H., Inoue,H.K., Komiya,Y., and Igarashi,M. (1998). Stimulation of L-type Ca2+ channel in growth cones activates two independent signaling pathways. J. Neurosci. Res. *51*, 682-696.

Olive,S., Dubois,C., Schachner,M., and Rougon,G. (1995). The F3 neuronal glycosylphosphatidylinositol-linked molecule is localized to glycolipid-enriched membrane subdomains and interacts with L1 and fyn kinase in cerebellum. J. Neurochem. *65*, 2307-2317.

Pfenninger,K.H. (2009). Plasma membrane expansion: a neuron's Herculean task. Nat. Rev. Neurosci. *10*, 251-261.

Pfenninger,K.H., Ellis,L., Johnson,M.P., Friedman,L.B., and Somlo,S. (1983). Nerve growth cones isolated from fetal rat brain: subcellular fractionation and characterization. Cell *35*, 573-584.

Phillips,M.D. and Thomas,G.H. (2006). Brush border spectrin is required for early endosome recycling in Drosophila. J. Cell Sci. *119*, 1361-1370.

Pielage,J., Fetter,R.D., and Davis,G.W. (2005). Presynaptic spectrin is essential for synapse stabilization. Current Biology *15*, 918-928.

Ramesh,V. (2004). Merlin and the ERM proteins in Schwann cells, neurons and growth cones. Nat. Rev. Neurosci. *5*, 462-470.

Robles,E., Huttenlocher,A., and Gomez,T.M. (2003). Filopodial calcium transients regulate growth cone motility and guidance through local activation of calpain. Neuron *38*, 597-609.

Rolf,B., Lang,D., Hillenbrand,R., Richter,M., Schachner,M., and Bartsch,U. (2003). Altered expression of CHL1 by glial cells in response to optic nerve injury and intravitreal application of fibroblast growth factor-2. J. Neurosci. Res. *71*, 835-843.

Sakurai,K., Migita,O., Toru,M., and Arinami,T. (2002). An association between a missense polymorphism in the close homologue of L1 (CHL1, CALL) gene and schizophrenia. Mol. Psychiatry *7*, 412-415.

Schlatter,M.C., Buhusi,M., Wright,A.G., and Maness,P.F. (2008). CHL1

promotes Sema3A-induced growth cone collapse and neurite elaboration through a motif required for recruitment of ERM proteins to the plasma membrane. J. Neurochem. *104*, 731-744.

Schmid,R.S., Pruitt,W.M., and Maness,P.F. (2000). A MAP kinase-signaling pathway mediates neurite outgrowth on L1 and requires Src-dependent endocytosis. J. Neurosci. *20*, 4177-4188.

Schmid,R.S., Shelton,S., Stanco,A., Yokota,Y., Kreidberg,J.A., and Anton,E.S. (2004). alpha3beta1 integrin modulates neuronal migration and placement during early stages of cerebral cortical development. Development *131*, 6023-6031.

Schneider,A., Rajendran,L., Honsho,M., Gralle,M., Donnert,G., Wouters,F., Hell,S.W., and Simons,M. (2008). Flotillin-dependent clustering of the amyloid precursor protein regulates its endocytosis and amyloidogenic processing in neurons. J. Neurosci. *28*, 2874-2882.

Schulte,T., Paschke,K.A., Laessing,U., Lottspeich,F., and Stuermer,C.A. (1997). Reggie-1 and reggie-2, two cell surface proteins expressed by retinal ganglion cells during axon regeneration. Development *124*, 577-587.

Seals,D.F. and Courtneidge,S.A. (2003). The ADAMs family of metalloproteases: multidomain proteins with multiple functions. Genes Dev. *17*, 7-30.

Sedgwick,S.G. and Smerdon,S.J. (1999). The ankyrin repeat: a diversity of interactions on a common structural framework. Trends Biochem. Sci. *24*, 311-316.

Sharma,P., Varma,R., Sarasij,R.C., Ira, Gousset,K., Krishnamoorthy,G., Rao,M., and Mayor,S. (2004). Nanoscale organization of multiple GPI-anchored proteins in living cell membranes. Cell *116*, 577-589.

Shipp,S. (2007). Structure and function of the cerebral cortex. Curr. Biol. *17*, R443-R449.

Sikorski,A.F., Sangerman,J., Goodman,S.R., and Critz,S.D. (2000). Spectrin (beta SpII Sigma 1) is an essential component of synaptic transmission. Brain Research *852*, 161-166.

Simons,K. and Ikonen,E. (1997). Functional rafts in cell membranes. Nature *387*, 569-572.

Simons,K. and Toomre,D. (2000). Lipid rafts and signal transduction. Nat. Rev. Mol. Cell Biol. *1*, 31-39.

Skene,J.H. (1990). GAP-43 as a 'calmodulin sponge' and some implications for calcium signalling in axon terminals. Neurosci. Res. Suppl *13*, S112-S125.

Stuermer,C.A., Lang,D.M., Kirsch,F., Wiechers,M., Deininger,S.O., and Plattner,H. (2001). Glycosylphosphatidyl inositol-anchored proteins and fyn kinase assemble in noncaveolar plasma membrane microdomains defined by reggie-1 and -2. Mol. Biol. Cell *12*, 3031-3045.

Takeichi,M. (1991). Cadherin cell adhesion receptors as a morphogenetic regulator. Science *251*, 1451-1455.

Thelen,K., Kedar,V., Panicker,A.K., Schmid,R.S., Midkiff,B.R., and Maness,P.F. (2002). The neural cell adhesion molecule L1 potentiates integrin-dependent cell migration to extracellular matrix proteins. J. Neurosci. *22*, 4918-4931.

Van den,B.M., Garner,B., and Koch,M. (2003). Neurodevelopmental animal models of schizophrenia: effects on prepulse inhibition. Curr. Mol. Med. *3*, 459-471.

Walsh,F.S. and Doherty,P. (1997). Neural cell adhesion molecules of the immunoglobulin superfamily: role in axon growth and guidance. Annu. Rev. Cell Dev. Biol. *13*, 425-456.

Wen,Z., Guirland,C., Ming,G.L., and Zheng,J.Q. (2004). A CaMKII/calcineurin switch controls the direction of Ca(2+)-dependent growth cone guidance. Neuron *43*, 835-846.

Williams,E.J., Doherty,P., Turner,G., Reid,R.A., Hemperly,J.J., and Walsh,F.S. (1992a). Calcium influx into neurons can solely account for cell contact-dependent neurite outgrowth stimulated by transfected L1. J. Cell Biol. *119*, 883-892.

Williams,E.J., Doherty,P., Turner,G., Reid,R.A., Hemperly,J.J., and Walsh,F.S. (1992b). Calcium influx into neurons can solely account for cell contact-dependent neurite outgrowth stimulated by transfected L1. J. Cell Biol. *119*, 883-892.

Wright,A.G., Demyanenko,G.P., Powell,A., Schachner,M., Enriquez-Barreto,L., Tran,T.S., Polleux,F., and Maness,P.F. (2007). Close homolog of L1 and neuropilin 1 mediate guidance of thalamocortical axons at the ventral telencephalon. J. Neurosci. *27*, 13667-13679.

Yan,Y., Winograd,E., Viel,A., Cronin,T., Harrison,S.C., and Branton,D. (1993). Crystal-Structure of the Repetitive Segments of Spectrin. Science *262*, 2027-2030.

Ye,H., Tan,Y.L., Ponniah,S., Takeda,Y., Wang,S.Q., Schachner,M., Watanabe,K., Pallen,C.J., and Xiao,Z.C. (2008). Neural recognition molecules CHL1 and NB-3 regulate apical dendrite orientation in the neocortex via PTP alpha. EMBO J. *27*, 188-200.

Yuan,J.Z., Ye,Q.F., Ming,Y.Z., Hang,Z.F., Zhao,L.L., Zhao,X.Y., Wang,M.M., Zhang,M.Z., Wen,Z.X., Zhu,S.H., and Wu,K. (2005). [Preoperation risk factor analysis in orthotopic liver transplantation with pre-transplant artificial liver support therapy]. Zhonghua Gan Zang. Bing. Za Zhi. *13*, 175-178.

Zagon,I.S., Higbee,R., Riederer,B.M., and Goodman,S.R. (1986a). Spectrin Subtypes in Mammalian Brain - An Immunoelectron Microscopic Study. Journal of Neuroscience *6*, 2977-2986.

Zagon,I.S., Higbee,R., Riederer,B.M., and Goodman,S.R. (1986b). Spectrin subtypes in mammalian brain: an immunoelectron microscopic study. J. Neurosci. *6*, 2977-2986.

Zhang,W., Trible,R.P., and Samelson,L.E. (1998). LAT palmitoylation: its essential role in membrane microdomain targeting and tyrosine phosphorylation during T cell activation. Immunity. *9*, 239-246.

Zimmer,W.E., Zhao,Y., Sikorski,A.F., Critz,S.D., Sangerman,J., Elferink,L.A., Xu,X.S., and Goodman,S.R. (2000). The domain of brain beta-spectrin responsible for synaptic vesicle association is essential for synaptic transmission. Brain Research *881*, 18-27.

Zimprich,F. and Bolsover,S.R. (1996). Calcium channels in neuroblastoma cell growth cones. Eur. J. Neurosci. *8*, 467-475.

IX ABBREVIATIONS

A	Alanine
Ab	Antibody
ADAM	A Disintegrin And Metalloproteinase
Amp	Ampicillin
ANK	Ankyrin
AP-2	Aaptor protein-2
APP	Amyloid precursor protein
APS	Ammonium peroxosulfate
ATP	Adenosine triphosphate
BH	Brain homogenates
bp	Base pair
BSA	Bovine serumalbumine
BG	Bergman glia
C	Cysteine
CAM	Cell adhesion molecule
CaMKIIα	Ca^{2+}/calmodulin-dependent protein kinase IIα

CD	Cytoplasmic domain
cDNA	Complementary deoxyribonucleic acid
CHL1	Close homologe of L1
ChFP	Cherry fluorescent protein
°C	Degree celcius
DMEM/F12	Dulbecco's Modified Eagle Medium: Nutrient Mixture F-12
DMSO	Dimethylsulfoxide
DNA	Deoxyribonucleic acid
DNAse	Deoxyribonuclease
DCS	Donor calf serum
EAAT4	Excitatory amino acid transporter 4
ECL	Enhanced chemiluminescence
ECM	Extracellular matrix
E.Coli	Escherichia coli
EDTA	Ethylenediamine tetraacetic acid
EGTA	Ethylene glycol tetraacetic acid
ELISA	Enzyme-linked immunosorbent assay

ERM	Ezrin-radixin-moesin
F	Phenylalanine
F-actin	Filamentous-actin
FAK	Focal adhesion kinase
Fc	Fragment crystallizable
FGF	Fibroblast growth factor*s*
FNIII	Fibronectin type III domain
g	g-force
G	Glycine
GAP-43	Growth associated protein 43
GAPDH	Glyceraldehyde-3-phosphate dehydrogenase
GC	Growth cone
GPI	Glycophosphatidylinositol
GST	Glutathione S transferase
GTP	Guanosine-5'-triphosphate
HBSS	Hank's banlanced salt solution
HEPES	2-(4-(hydroxyethyl)-piperazine)-ethane sulfonic acid

HRP	Horseradish peroxidase
I	Isoleucine
ICAM	Inter-cellulsr adhesion molecule
ID	Intracellular domain
Ig	Immunoglobulin
IgSF	Immunoglobulin superfamily
IPTG	Isopropyl-D-thiogalactopyranoside
kb	Kilo base pairs
kD	Kilo Dalton
LB	Luria bertani
µ	Micro (10^{-6})
m	Milli (10^{-3})
MAPK	Mitogen-activated protein kinase
MEK1/2	MAPK or Erk kinases 1/2
mRNA	Messenger ribonucleic acid
n	Nano (10^{-9})
NB-DNJ	*N*-butyldeoxynojirimycin

NCAM	Neural cell adhesion molecule
Ng-CAM	Neuron-glia cell adhesion molecule
NP-1	Neuropilin-1
OD	Optical density
PAGE	Polyactrylamide gel eletrophoresis
PBS	Phosphate bufferd saline
PCR	Polymerase chain reaction
PH	Pleckstrin homology
PKC	Protain Kinase C
PMSF	Phenylmethylsulphonyl fluoride
PTPα	Protein tyrosine phosphatase α
Q	Glutamine
RNA	Ribonucleic acid
rpm	Rotations per minute
RPTPα	Receptor-like protein tyrosine phosphatase α
S	Serine
Sema 3A	Semaphorin 3A

SDS	Sodium dodecyl sulfate
SDS-PAGE	Sodium dodecyl sulphate poly acrylamide gel electrophoresis
SH3	Src homology 3
SNARE	soluble N-ethylamleimide-sensitive factor attachment protein receptor
TBS	Tris buffer saline
TEMED	N,N,N',N',-tetramethylethylene diamine
V	Volts
VCAM	Vascular cell adhesion molecule
VDCC	Voltage-dependent calcium channel
v/v	Volume per volume
w/v	Weight pre volume
Y	Tyrosine

X ACKNOWLEDGEMENTS

I end this thesis with the acknowledgments. I would like to warmly thank Prof.Mellita Schachner for ‘‘recruiting’’ me to the institute of ZMNH and introducing to me the CAMs – very lovely molecules, especially CHL1. I really admire her devotion and enjoyment in science. The entire project cannot be finished without her support, discussion and guidance during these years.

I am especially grateful to Dr. Vladimir Sytnyk and Dr.Iryna Leshchyns’ka, who supervised the whole project, for excellent scientific-training, fruitful and patient discussion, valuable ideas and constant support. I am impressed by their energetic and productive in science.

I would like to thank Prof. Aleksander F Sikorski from university of Wroctaw for kindly providing me the purified brain spectrin.

I also would like to thank all my friend and colleagues for their support in different ways. All the lovely images of these nice people compose my colorful PhD life in ZMNH. Special thanks to old Joe, an ordinary non-scientist with extraordinary wisdom.

A lots of thanks to my family, my parents, for bringing me to this world and supporting me with all their hearts; my dear husband, wei, for his understanding, supporting, being a nice friend and considerate ‘‘supervisor’’ in my life.